[paper: nhess-2019-67]

Old Title: **Assessment of potential seismic hazard for sensitive facilities by applying seismo-tectonic criteria: an example from the Levant region**

New title: **Assessment of seismic sources and capable faults through hierarchic tectonic criteria: implications for seismic hazard in the Levant**

Matty Sharon et al.

asagy@gsi.gov.il

We would like to thank the three anonymous reviewers for their in-depth review of the manuscript and their constructive and important comments. Following the comments, we have thoroughly revised the article. The manuscript title, introduction, discussion and conclusion chapters were rewritten. We provide below detailed replies to the reviewer's comments and indicate how and where changes were made in the revised manuscript. Please note that the lines we refer to, are at the manuscript submitted as a different file.

Referee #1

1) "the title of the manuscript: "Assessment of potential seismic hazard for sensitive facilities" is misleading and erroneous. The paper does not contain any hazard analysis, or a comparison to existing hazard assessments for the area"

Author's response:

following the reviewer comment we wrote a new title that reflect this study more accurately. New title: "Assessment of seismic sources and capable faults through hierarchic tectonic criteria: implications for seismic hazard in the Levant "

2) "There is no discussion on how these results will affect hazard or any direct practical connection between the presented analysis and hazard calculations."

Author's response: Although our new title and introduction now describe that hazard calculations are not part of this study, we added a new section that discusses the applications for hazard evaluations (Sec. 7.1 – lines 442 - 494). The map and the slip rates of Fig. 5, as well as the local seismic intensity that we analysed here, are fundamental inputs for ground shake models and acceleration maps. The capable faults map, on the other hand, can be used for choosing potential cites for planning special facilities. Defining faults parameters, maps and local seismic characters, as we done here, are the first steps in hazard evaluations. We further emphasise that the two maps (Figs. 5, 7) enable defining the relevant faults necessary for regional hazard models, but they do not necessarily replace local maps of other faults that required in some standards, when siting in a specific location is considered.

3) “"surface rupture and ground shaking are intermixed as ‘seismic hazard’ and the fault mapping is presented as the answer for both. However – ground shaking and surface rupture are two very different types of hazard. They require different considerations in planning, etc. Is it wise to treat both as one? "

Author’s response: Following the reviewer comment, we declare in the introduction (within lines 38-58) that we generate a database of faults that is relevant for several seismic hazards. We demonstrate how we categorise faults for two specific different requirements: one that is aimed to be used in ground shaking models, and the other for siting critical facilities or special infrastructures. We however do not evaluate seismic hazard in this paper, as well as site specific requirements. These are beyond the scope of this paper.

4) "What is very much missing is a thorough discussion on the relationship between the two types of analysis (seismicity based criteria and faulting) – how do you suggest combining the two datasets that you have created ?
(1) In places where they overlap (e.g. DST), should they both be accounted for in the hazard analysis? If not – what should be the interaction ? (2) In places where they do not overlap (e.g. east Sinai), do you ignore the seismicity criterion? Do you add a ‘seismogenic zone’? What is your suggestion? (3) What about places in which the kernel density is zero? Do you think there is really a zero probability of an earthquake occurring there, keeping in mind the short time window used for the kernel density?
These are all very important hazard decisions, which this paper does not address.”

Author’s response: The products of the seismologic analysis are applied differently in the two maps (Figs. 5, 7). We design a seismicity-based criterion that is based on the distribution of two parameters: the earthquake kernel density and the seismic moment kernel density. Faults that are located beyond this pattern are not part of the faults of Fig. 5. The seismological character of a zone is considered as part of criterion for the map in Fig. 7. The success of this selection is further reinforced by the match between the geological-categorised faults and the seismicity criterion (Fig. A4). This subject is discussed in Sec. 7.1 (within lines 449-464). However, if this comment refers to the aspect of utilising the ‘gridded seismicity’ (i.e. the grid-based distribution of the seismicity parameters) as an independent database for both surface rupture and ground motion hazards, we emphasise that we focus on generating databases of faults and not on utilising the seismicity as an independent source for hazard evaluations. Therefore, we did not discuss this issue. We now clarify this in the introduction. However, we add a section that discuss the applications of our different analyses to seismic hazard evaluation, included possible usages of the ‘gridded seismicity’ for hazard evaluations (lines 473-476).

5) “Seems to me that your mapping methodology is more appropriate for surface rupture analysis than for shaking (which also takes into account faults that did not rupture the surface, etc.). Please be more accurate in describing your contribution and its expected useage.”

Author’s response: A discussion focuses on our methodology and its applications for both surface rupture and ground shaking hazard analyses is now written in Sec. 7.1 (particularly relevant to this comment are lines 449–451; 465–476). Subsurface faults were considered for capable faults if they are the continuation of categorised faults or if there is information that they offset Quaternary formations. On the other hand, for the main seismic sources, they are neglected. Indeed, when a local siting process is applied (both for rupture surface and for shaking), information on local fault which are not categorised in our regional analysis should be taking into account.

6) " The abstract says: "our analysis allows revealing the tectonic evolution of a given region". Therefore, it is expected that you will show this later in the results. Nowhere in the paper do you "reveal" anything new about the tectonic evolution that wasn’t already known. Therefore – please clarify what exactly is new knowledge gained by this paper? This is typically done by comparing to previous studies or discussing the specific contribution presented in this study.”

Author’s response: We changed this sentence in the abstract. We also added a new section (Sec. 7.2 in our new discussion – lines 496 - 537), a new figure in the appendix (A4) and a conclusion (No. 6, lines 575 - 583) that focuses on the implications for local tectonics and slip dynamics.

7) “Table 1: title of 2nd column should be ‘slip rate’ rather than ‘strike-slip’. Also, seems to me that the first slip rate that is mentioned for the Yammuneh fault is too low. It references Gomez 2007 but I think his numbers are higher. How exactly did you reach 2.8 mm/yr?”

Author’s response: Numbers are for lateral slip rates – we now changed ‘Lateral slip rate’ (Table 1 is in line 845). 2.8 mm/yr in Table 1 was a mistake and is now deleted.

8) “Conclusion number 3 is not exactly a conclusion. It’s an opinion, or a suggestion. While important and relevant, it isn’t based on any analysis or data and hence cannot be presented as a conclusion of the paper. Please rephrase.”

Author’s response: following the three reviewers’ comments we rewrote the conclusion’s section (lines 539 – 583). Specifically, we also rephrased conclusion 3 (now is listed as conclusion 4 – lines 556 – 565).

9) ”Line 296 – the symbol Vs is typically used for shear-wave velocity in the geotechnical earthquake engineering community. I suggest using something else for slip rate.”

Author’s response: We no longer use this symbol. Instead, we now use a simple “range” character (e.g. a – b mm/yr) (e.g. lines 302-303).

10) ” Line 454 – remove ‘many’ “

Author’s response: Removed

11) ” Line 455 – ‘could have entered the map’ rather than enter “

Author’s response: Corrected

12) “Line 460 – ‘Quaternary activity exists’.”

Answer: Corrected

13) “Line 462 – siting of what? What is siting? Why is this related?”

Author’s response: We rewrote the entire section (this subject is discussed in Sec. 7.1), and also added relevant parts in the introduction (e.g. lines 43 – 52).

Referee #2

1) “I find nothing new in terms of methodology.”

Author’s response: Indeed, seismo-tectonic criteria for categorising faults were previously applied in seismic hazard analyses. However, in addition of classifying hazardous faults by the recency of faulting or their recurrence intervals:

a) We design a seismicity-based criterion that use the distribution of two parameters:

the *earthquake kernel density* and *seismic moment kernel density*. This criterion is reinforced by the match between the geological-categorised faults and the seismicity criterion (Fig. A3). b) Seismic sources for ground shaking maps are considered only faults that are satisfied both geological and seismological criteria. This is significant when slip rates are mostly unknown (as in Sec. 5.2).

c) The internal hierarchic categorisation of faults, in both maps, enable weighting different faults when hazard evaluation is applied.

We now discuss this in the new section 7.1.

2) “If the goal of this research is to describe a new approach for seismic hazard assessment for critical facilities, this goal is not achieved”

Author’s response: We agree and following the comment of the Anonymous Referee #1, we have already changed the title of this paper, so it is no longer “assessment of potential seismic hazard”.

3) “First of all, the manuscript deals with Israel region, and I do not see how this approach can be exported to other seismo-tectonic settings.”

Author’s response: We now specifically discuss the universal aspects of our analysis in Sec. 7.1 (also, please see our response to Referre #1).

4) “Even for the Israel region, the manuscript does not address the most critical issue , that is the potential for M>6 earthquakes and accompanying surface faulting in the areas that are not close to the Dead Sea Transform, such as the Sinai peninsula and the coastal region along the Mediterranean Sea. This topic should be discussed based on the data presented in the manuscript. Several critical facilities in the Levant region are located, or are in the process of being located, relatively far from the DST. The reason is obvious, the seismic hazard along the DST is clearly very high, and whenever this is possible sites along the DST are immediately discarded during any process of siting for high risk plants and infrastructures. The manuscript should be revised in other to take into account ground motion and ground rupture hazard evaluation in the less active areas.”

Author’s response: The potential of capable faults, which are not part of the main seismic sources, is indeed not discuss in this paper. The aim of this paper was to separate the capable faults from other faults and categorise them. The next step should be generating statistic and/or deterministic methods for defining the safety distances for any specific siting. This is beyond the scope of the paper.

5) “Moreover, the criteria used for interpreting Quaternary faults as capable faults are not very clear. Some marginal fault of the DST is interpreted as “source of M>6 earthquakes”, some other as “capable fault”. This is misleading. If the definition of capable fault is “a fault with significant potential for earthquake surface faulting”, a fault capable of surface faulting is by definition a source for M>6 earthquakes; of course, assuming that hypocentral depth is shallow crustal, as clearly stated in Wells and Coppersmith (1994).

Author's response: The faults in the different maps (Figs. 5, 7) are all capable to generate large earthquake (M>6). However, the time frame, slip rates and seismological activity are different. Specific definitions are presented and explained in the beginning of Sec. 5 and Sec. 6.1 "Framework and principles".

6) "If the problem is the probability of surface faulting events, there should be a discrimination in terms of seismo-tectonic setting. Along the DST, that is a very active structure, the time window to be considered for capable faults should be relatively short, like the Holocene, or 13 kyr BP (the Lisan Lake shoreline criterion used in the regulatory framework for Israel). For the Sinai region, the Quaternary criterion is much more reasonable. The choice of different time-windows for fault capability takes into account the regional plate tectonic setting of the Levant. Using the Quaternary time windows for the whole region does not."

Author's response: Basically, we think that using longer time intervals for defining capable faults, as an increasing distance from active sources, can be misleading. Even using the "earthquake cycle" period for defining capable faults, as suggested by Machette (2000), might be sustained only when large regimes are compared. We suggest that the combination of the tectonic regional field (stress field orientation, displacement rates) and the level of the geological information (stratigraphy, map resolutions) should determine the relevant time frame for capable faults (see Sec. 6.1).

7) "In fact, from the historical seismicity perspective, all along the Dead Sea Transform you have a sequence of large events with epicentral intensity X or XI in the MM scale. This implies that virtually every fault along the DST might have been reactivated by coseismic surface faulting in the past 2000 years or so. This macroseismic evidence should be properly taken into account."

Author's response: The estimated intensity of past earthquakes is translated into magnitudes. We already considered the interpretation of historical earthquakes for estimating the maximum magnitude at the end of Sec. 5.1 (lines 316 - 318). These interpretations and the related slip rates are sufficient for the purpose of this paper.

8) "In Figure 7 from the manuscript, there is no Quaternary fault East of the DST, and very little West of the DST. Is this a real feature, or is controlled by the completeness and resolution of the instrumental and geological database?"

Author's response: Indeed, the capable fault map does not include faults in neighboring countries. We now clearly this in Sec. 6.1 (lines 387-388). Also see our geological database in Sec. 3.

9) "The manuscript describe and discuss the available instrumental earthquake catalog. No discussion and description is available about the historical catalog. Integration between

instrumental and pre-instrumental datasets is fundamental for seismic hazard assessment. Please discuss."

Author's response: We regard the information of historical earthquakes for estimating the maximum magnitude. Further considerations are beyond the scope of this paper. We now changed the title of our manuscript so it is no longer "seismic hazard assessment".

10) "A few papers cited in the text are not included in the list of references; find this in the attached annotated manuscript."

Author's response: Fixed

11) "Please also note the supplement to this comment: https://www.nat-hazards-earthsyst-sci-discuss.net/nhess-2019-67/nhess-2019-67-RC2-supplement.pdf"

Author's response: We responded to the comments in this pdf file, and clarify associated issues in our new version of the manuscript.

Please also note the supplement to this comment:

https://www.nat-hazards-earth-syst-sci-discuss.net/nhess-2019-67/nhess-2019-67-AC2-supplement.pdf

Referee #3

1) "1- The title is irrelevant as I could not see a comprehensive seismic hazard analysis, unless the author consider defining the active and capable faults (seismic source model) is a complete hazard assessment process. It is very important component in any seismic hazard study, but it is not the entire process."

Author's response: We accept this comment and have changed the title of this paper. New title: "Assessment of seismic sources and capable faults through hierarchic tectonic criteria: implications for seismic hazard in the Levant"

2) "2- Regarding the exclusion of a very important event Md 5.8 1993 due to unreliable location, please show how much the location is uncertain. Compare this with the clear uncertainty in location around the Gulf of Aqaba."

Author's response: The event Md 5.8 1993 is indeed important, but it occurred in the most seismically active zone of the Gulf of Elat (Aqaba), in such distance from our database of mapped faults, that it would not have any impact on the current results. Since the focus in this paper is the mapping of faults, further details such as error issues of a specific earthquake, which has no impact on the mapping of any fault, is irrelevant. We now clarify this though (lines 189-191).

3) "3- Please show how many circles are included in your calculations and the weight of each circle"

Author's response: The 'circles' were given as an illustration, as mentioned in the text. However, we now see this illustration might be confusing, so we rephrase (lines 211-212)

the continuation of the last comment: "and why did you select (calculate) such weight."

Author's response: see lines 213-218.

4) "4- It seems that the catalog contains the aftershocks of large earthquakes, please show the role of these aftershocks as they are not due to primary tectonic movements. What is the situation if these aftershocks are removed from the calculations of earthquake kernel density distribution?"

Author's response: Indeed, the catalogue contains aftershocks. As already mentioned, the focus of this paper is the mapping of faults, based on the suggested methodology of hierarchic seismo-tectonic criteria. Showing the exact role of the aftershocks, and the situation if they are removed from the calculation, is a different topic. We also note that aftershocks may be also associated with reactivation of faults and even with surface ruptures, so they should not be neglected in a seismicity-based criterion for a capable fault map.

5) "5- For many faults the slip rate is provided based upon geologic or GPS surveys. Such slip may contain a creep component in addition to the seismic one. The role of creep should be addressed for all active faults as it could be a source of large uncertainty."

Author's response: We had already addressed the issue of evidences for a creep component: see discussion (lines 505-510) and Table 1 (lines 845, 850):

6) "5- With the large periods of quiescence observed frequently along many parts of DST, 35 years of instrumentally recorded seismicity are very short to reflect the active tectonics accurately. This period should be extended using robust historical records."

Author's response: We regard the information of historical earthquakes for estimating the maximum magnitude (lines 316-318), and also consider slip rates deduces from field measurements of much longer periods (see Table 1, and also figure A3 we now added).

7) "6- Although the seismicity and earthquake kernel density distribution show high seismicity to the east of the Gulf of Aqaba, neither active nor capable faults are inferred at this area."

Author's response: As we already noted (see response to Referee #2), except for few exceptions (see Sec. 3 and 6), the capable fault map does not include faults in neighbouring countries. Specifically, we mapped a few faults within the Gulf of Aqaba that we define as 'main seismic sources' (see Sec. 5). This is sufficient for our purposes, which we now describe more clearly throughout the paper.

8) "7- Abbreviations should be explained at their first appearance in the text (e.g. LRB). Some abbreviations has no explanation (QFMI)."

Author's response: Corrected.

9) "8- Minor comments a) Line 54 contains two fullstops, please remove one of them. b) Arrange references in line 116 in a chronological order. c) Sentence in lines 147 and 148 needs reference. d) Change figure 4 into Fig. 4 in line 258. e) Change demonstrates into demonstrate in line 282. F) Change is represents in line 366 into represents. g) Rewrite lines 408 to 411 as it is really so difficult to be followed. h) Remove many in line 454. i) Sea of Galilee should be shown on a map. j) ARF is repeated in Fig. 7. k) All the maps lack to the North Direction Indicator."

Author's response:

a) Two full-stops are now removed in all parts of the manuscript. b) Corrected (now in lines 122-123). c) We now add a new reference (now in line 155). d) Corrected (now in line 264): e) Corrected (now in line 288). f) Corrected (now in line 376). g) We rephrased (now in lines 417-420). h) Already removed due to comment by Anonymous Reviewer #1. i) We added marks for the Dead Sea Basin (DSB) and for the Sea of Galilee (SG) to Figure 1. j) Fixed. k) All our maps are orientated such that the north is directed upwards. We do not think that a North arrow is necessary.

Assessment of ~~potential seismic hazard for sensitive facilities by applying seismo-~~seismic sources and capable faults through hierarchic tectonic criteria: ~~an example from~~implications for seismic hazard in the Levant ~~region~~

Matty Sharon[1,2], Amir Sagy[1], Ittai Kurzon[1], Shmuel Marco[2], Marcelo Rosensaft[1]

1. Geological Survey of Israel, Jerusalem 9371234, Israel

2. Porter School of the Environment and Earth Sciences, Tel Aviv University, Tel Aviv 6997801, Israel

Correspondence to: Amir Sagy ~~(asagy@gsi.gov.il)~~(asagy@gsi.gov.il)

Abstract

We present a methodology for mapping faults that constitute a potential hazard to structures, with an emphasis on ~~special~~ground shake hazards, and on surface rupture nearby critical facilities such as dams and nuclear power plants. The methodology categorises faults by ~~hierarchical~~hierarchic seismo-tectonic criteria, which are designed according to the degree of certainty for recent activity and the accessibility of the information within a given region. First, the instrumental seismicity is statistically processed to obtain the gridded seismicity of the *earthquake density* and the *seismic moment density* parameters. Their spatial distribution reveals the zones of the seismic sources, within the examined period. We combine these results with geodetic and pre-instrumental slip rates, historical earthquake data, geological maps and ~~other sources~~aerial photography to define and categorise faults that are likely to generate significant earthquakes (M ≥ 6.0). Their mapping is fundamental for seismo-tectonic modelling and for PSHA analyses. In addition, for surface rupture hazard, we create a database and a map of Quaternary capable faults, by developing criteria according to the regional stratigraphy and the ~~seismotectonic~~ tectonic configuration. The relationship between seismicity, slip dynamics, and fault activity through time, is an intrinsic result of our analysis that allows revealing the ~~tectonic evolution~~dynamic of ~~a given~~the deformation in the region. The presented methodology

expands the ability to differentiate between subgroups for planning or maintenance of different constructions or for research aims, and can be applied in other regions.

1. Introduction

The global population growth and the establishment of sensitive facilities, such as nuclear power plants or dams~~ have been raising~~, increase the seismic risk to higher levels and ~~entail the need for a~~require profound understanding of the seismic hazard (e.g. Marano et al., 2010). Probably the most famous example is the destruction of the Fukushima nuclear power plant by the tsunami~~ waves~~ caused by the 2011 $M_w = 9.0$ Tohoku-oki earthquake, which has been affecting an extensive region ever since.~~ Identifying and characterising the regional seismic sources and their potential hazard is therefore fundamental for siting and designing of potential facilities, and for risk management. Additionally, in the case of infrastructures, the hazard also includes surface rupture in close proximity to the construction. The goals of this study are to define the regional main seismic sources, presuming that these are the sources that are likely to generate the most significant earthquakes in the near future, and to minimise the likelihood of surface rupture at the underlying infrastructure of sensitive facilities.~~

A basic step in seismic hazard evaluation is defining and characterising faults that constitute a potential hazard. Because earthquakes are stochastic processes that trigger different hazards (such as ground shaking, tsunamis, landslides, liquefaction and surface rupture) and the planning of different infrastructures requires different safety standards, mapping and categorising hazardous faults is generated according to specific requirements.

In this paper, we present a methodology for mapping and categorising faults, which can be applied for the evaluation of different seismic hazards. To generate our maps and to classify the faults in them, we combine seismological analysis with geologic and geodetic information. The methodology is implemented for generating regional maps of the "main seismic sources" and of "capable faults". The former are the regional faults that should be considered for ground shaking models and Probabilistic Seismic Hazard Analysis (PSHA), and the latter constitute surface rupture hazards that should be considered for siting facilities with environmental impact, such as dams and nuclear plants, or other vulnerable facilities. We apply hierarchic criteria for categorising faults according to the specific hazard.

We demonstrate our methodology for the Israel region, a seismically-active zone mainly affected by the Dead Sea Transform fault system (DST; Fig. 1). First, we determine the main seismic sources in Israel and its vicinity, focusing on faults that are likely to generate significant earthquakes. Subsequently, we present the procedure to determine and map faults that constitute a potential hazard of surface rupture for sensitive facilities. We design the criteria according to the likelihood of surface rupture along specific faults.

Despite the limited duration of the instrumental record, it constitutes one of the main direct evidence of fault activity in the current tectonic configuration. Probabilistic analyses of seismicity can constrain fault locations, kinematics and activity rates (e.g. Woo, 1996; Atkinson and Goda, 2011). Moreover, the Gutenberg-Richter empirical law ~~allows assessing~~can aid to assess the frequency of ~~medium to~~ strong ~~earthquakes~~shocks by extrapolating ~~low~~lower-magnitude earthquakes. Since surface ruptures are usually associated with M $\geq$ ~6.0 (Wells and Coppersmith, 1994; Stirling et al., 2002), the concentration of seismicity along faults ~~highly~~strongly suggests that surface ruptures occurred in the recent geological history. However, due to the scarcity of large earthquakes in the instrumental era, complementary information is required for further constraining the location of the main sources of significant earthquakes, and for characterising them. ~~.~~This information can come from archaeological and paleo-seismological investigations, and from historical documents (~~e.g.~~ Ambraseys, 2009; Agnon, 2014; Marco and Klinger, 2014; Zohar et al., 2016). Geodetic measurements of relative displacements and velocities provide further crucial kinematic information (Baer et al., 1999; Hamiel et al., 2016; 2018a~~;~~ ~~2018b~~, b).

Detailed geological investigation of faults ~~can~~ further ~~extend~~extends the necessary information, in particular for long-term activity. ~~In terms of~~From seismic hazard perspective, faults that were active in the recent geological periods have a ~~larger~~higher probability for future faulting~~, compared with other faults.~~. Field relations between faults and geological units, as revealed in geological maps, can ~~force constraints on~~constrain the location, timing and the amount of offset of the relevant faults. However, these evidences are limited to places where faults ~~have field relationships with~~cross or abut young geological formations~~.~~ and landforms. Since the spatial distribution of ~~such~~young formations can be limited, additional criteria are required for mapping potentially hazardous faults.

~~In this paper we incorporate independent datasets to produce a variety of essential products for seismic hazard evaluation, including surface rupture and ground motion. We demonstrate it for the Israel region, a seismically-active zone mainly affected by the Dead Sea Transform fault system (DST; Fig. 1). We first determine the main seismic sources in Israel and its vicinity, focusing on faults that are likely to generate intermediate to large earthquakes. Subsequently, we present the process utilised to determine and map faults that constitute a potential hazard of surface rupture for sensitive facilities. We design the criteria according to the likelihood of surface rupture along specific faults.~~

2. Tectonic settings

The continental crust in the region of Israel was formed during the Pan-African orogeny of Late Precambrian age, and was later subjected to alternating periods of sedimentation and erosion during the Paleozoic (Garfunkel, 1998). Continental breakup and the establishment of passive margins along the Tethys-Mediterranean coast of the Levant occurred during the Triassic-Jurassic time. Widespread carbonate platform developed during the mid-Cretaceous. Since the Upper Cretaceous, the region was subjected to ~WNW compression of the Syrian-Arc system, deforming the sedimentary sequence into a series of asymmetric folds, strike-slip faults, and monoclines (Eyal and Reches, 1983; Sagy et al~~,~~., 2003). Regional uplift began from the end of the Eocene and the area was intermittently exposed to erosional processes (Picard, 1965). The African-Arabian plate broke along the suture of Gulf~~-~~ of~~-~~ Aden~~,~~ - Red Sea during the Miocene, generating the Suez rift and the DST which separate the Sinai sub-plate from the African and the Arab plates (Fig. 1). ~~-~~The Suez rift, however, has shown relatively minor signs of deformation since the end of the Miocene (Garfunkel and Bartov, 1977; Joffe and Garfunkel, 1987; Steckler et al., 1988~~), while the DST system remains the most active tectonic feature in the area.~~). In the ~~Easternmost~~easternmost Mediterranean Sea, the ~~current plate boundary~~ deformation ~~is taking place~~concentrates along the convergent Cyprian Arc (Fig. 1), where the Anatolian plate overrides the plates of Africa and Sinai (e.g., Mckenzie, 1970).

~~The~~ With Quaternary slip rates of 4–5 mm/yr, evaluated from geological reconstructions, paleo-seismological and geodetic measurements (e.g. Garfunkel, 2011; Marco and Klinger, 2014; Hamiel et al., 2018a, b), the 1000-km DST is the largest fault system in the ~~east~~ eastern Mediterranean region (Fig. 1). Its northern section crosses northwest Syria in a N-S orientation; several recent large earthquakes were attributed to this section during the past two millennia (Meghraoui et al., 2003). The middle section of the DST is ~~a~~the Lebanon restraining bend (LRB; Fig. 1), characterised by transpression deformation (Quennell, 1959). ~~The~~This section is branched to a few segments that transfer the main component of the strike-slip motion in Lebanon area (Gomez et al., 2003; 2007). The Israel region is located along the southern section of the DST but seismically it is also affected by the activity of the middle part.

The southern part of the DST (Fig. 1) is dominated by a sinistral ~~motion of approximately ~5 mm/yr, summing up to ~105-km of left-lateral~~ displacement of ~105-km over ~~a period of 15~~the last ~16-20 million years (~~e.g.~~Quennell, 1959; Garfunkel, 1981; 2014). It is marked by a pronounced 5–25 km wide topographic valley, mostly with uplifted flanks, bordered by normal faults that extend along the valley margins. The lateral motion occurs on longitudinal left-stepping strike-slip and oblique-slip fault segments. The strike -slip segments delimit a string of en-echelon arranged rhomb-shaped narrow and deep releasing bends that are associated with orthogonal separation of the transform flanks on the surface~~, which may well extend beneath the crust~~ (Garfunkel, 1981; Garfunkel and Ben-Avraham, 2001; Wetzler et al., 2014). The seismic potential ~~was~~is clearly expressed by the 1995 $M_w = 7.2$ Nuweiba earthquake in the Gulf of Elat (Aqaba), the largest seismic event documented instrumentally on the DST~~. Historical~~, as well as by historical and prehistorical large earthquakes ~~are also well documented~~ (e.g. Amit et al., ~~Marco, 2008~~2002; Marco et al., 2005; Marco, 2008~~Amit et al., 2002). The slip rates along the DST vary between different fault segments and time resolutions, but converges at about 4–5 mm/yr, approximately the same values obtained by GPS measurements (Marco and Klinger, 2014; Hamiel et al., 2018a; 2018b~~). Deep-crust seismicity is significant along the southern part of the DST in correlation with areas of low heat flow, particularly ~~along~~in the Dead Sea ~~Basin~~basin, probably indicating a cool and brittle lower crust (Aldersons et al., 2003; Shalev et al., 2007; 2013).

The Sinai sub-plate south to Lebanon displays some~~ amount of~~ internal deformation expressed by a few fault systems, which are associated with Quaternary activity. The Carmel-Tirza Fault zone (CTF; Fig. 1) consists of a few normal and oblique fault segments generally striking SE-NW~~-SE~~. The system is characterised by low heat flow and by relatively deep seismicity (Hofstetter et al., 1996; Shalev et al., 2013). The CTF divides the ~~Israel-~~Sinai sub-plate into two tectonic domains (Neev et al., 1976; Sadeh et al., 2012) where the southern part is assumed to be relatively rigid, while northward, normal faults orientated E~~–~~-W generate S-N~~-S~~ extension expressed by graben and horst structures (Ron and Eyal, 1985). South of the CTF, E-W to WSW-ENE trending faults constitute the Sinai – Negev shear belt (SNB in Fig. A4). Geological evidences reveal different activity phases of mainly dextral slip with some vertical motions, also during the Neogene (Bentor and Vroman, 1954; Bartov, 1974; Zilberman et al., 1996; Calvo and Bartov, 2001). The DST post-dates the SNB, but their present tectonic interaction is not entirely clear (Garfunkel, 2014).

3. Geological Database

The database of faults that were active in the recent geological history is mainly based on high-resolution geological maps. As of January 2019, 71 geological map sheets in the scale of 1:50,000 are available for this study, out of the 79 sheets required to cover the whole state of Israel (Fig. A1). The 1:200,000 geological map of Israel (Sneh et al., 1998) is utilised where 1:50,000 data are absent. Included also are faults defined as active or potentially active during the last 13,000 years, for the Israel Standard 413 (building code) "Design provisions for earthquake resistance of structures" (Sagy et al., 2013). In addition, some faults~~ that~~, which have not been mapped (or not updated yet) crossing Quaternary units in the geological maps, are marked here as Quaternary faults based on evidence presented in scientific publications, reports, and theses (see Table A1).

The establishment of Quaternary formation database (Table A2~~),~~) to constrain fault activity in this study is complicated due to poorly constrained geochronology of some of the formations. In some cases, the age uncertainty is in the order of millions of years. Moreover, the boundary Pliocene-Pleistocene~~-Pliocene~~ (Neogene-Quaternary) was shifted in 2009, from ~1.8Ma to ~2.6Ma~~.~~ (Gibbard et al., 2010). Thus, some formations that had previously been assigned Pliocene age became part of the Pleistocene. Therefore, geological periods attributed to some formations, mentioned in pre-2009 publications, might mislead. Many stratigraphic charts of the pre-2009 geological maps are outdated. Furthermore, as recent research provides better geochronological constraints, the most up-to-date information is required in order to correctly select Quaternary formations. In Appendix 1 (Table A1) we present references to Quaternary faults that cannot be directly deduced from the geological maps.

Beside the surface traces of mapped faults, offshore and subsurface continuation of faults, as well as faults extending beyond the Israeli borders were added to the database (Table A3). The latter are limited to the extensions of mapped faults that are within Israel, and/or the main DST segments. The criteria for selecting these faults are discussed in section 6.

4. Seismological analysis

We analyse the spatial distribution of seismic events in order to reveal the regional seismic pattern, which helps to define the main seismic sources and develop an independent criterion for Quaternary active faults. ~~In order~~So as to define the seismicity-based criterion, we ~~designe~~design seismic criteria that are based on the distribution of two parameters that are, to a large extent, independent: the ~~*Earthquake Kernel Density*~~*earthquake kernel density* and the ~~*Seismic Moment Kernel Density*~~*seismic moment kernel density*. We demonstrate the methodology and then present the results below.

4.1 Dataset

We use an earthquake catalogue from 1.1.1983 until 31.8.2017 within 28°N – 34°N and 33°E – 37°E, recorded by ~140 stations whose distribution has changed in time and space. Most of the data are from the Israel Seismic Network (ISN), the Comprehensive Nuclear Test-Ban Treaty (CTBT), and the Cooperating National Facility (CNF). Some additional data were incorporated from other regional networks: GE, GEOFON global network of Deutsches GeoForschungsZentrum, Potsdam (GFZ), Jordanian Seismic Observatory (JSO), and the seismic network of Cyprus (CQ). These earthquakes, which have been monitored by the Seismological Division of the Geophysical Institute of Israel, comprise a catalogue of ~17,600 earthquakes. They were relocated (Fig. 2) to generate a new catalogue with more precise locations of hypocentres (Wetzler and Kurzon 2016). As part of the relocation process, ~900 earthquakes were excluded for various reasons, e.g., events that were recorded by less than 4 stations; large location errors (including the $M_d = 5.8$ 1993 event in the Gulf of Elat~~).~~, which anyhow does not affect our marking of faults since it was nucleated outside our high-resolution geological data). Before 1983 the locations are less reliable. Hence, the relocated catalogue consists of ~16,700 events of $0.1 \leq \mathrm{M} \leq 7.2$ (Fig. 2). Earthquakes with unknown magnitudes received a default value of $\mathrm{M} = 0.1$. The magnitude and the location of the $\mathrm{M_w} = 7.2$ 1995 Nuweiba earthquake were fixed according to Hofstetter et al. (2003).

In order to assess the applicability of the following seismic processing and analysis, we define the network coverage area as the zone in which the hypocentres are relatively well-constrained. This is examined and determined here as the polygon that covers all seismic stations that recorded at least 350 arrivals, and consists of the smallest number of polygon-sides that link between the stations (Fig. A2 in Appendix 2).

4.2 Spatial data processing

In order to quantitatively characterise the regional seismicity and associate the earthquakes with mapped faults we examine two parameters: a) *earthquake kernel density* and b) *seismic moment* (M_0) *kernel density*. Both parameters are obtained through the following spatial data processing. A regional scan is carried out in a 0.5-km interval 2D grid, in the horizontal coordinates. For each grid point, both parameters are calculated ~~for the~~utilising all recorded events within a 6-km ~~distance of the grid point~~radius. The parameters are calculated based on the kernel density estimation as an approach to obtain the spatial distribution through a probability density function, using the distance to weight each event from a reference point (each grid point~~). The weighting can be illustrated as many circles of up to 6-km radius that surround a~~, the common centre ~~(every grid point).~~

~~The circle~~ of its adjacent events). This circular-shape based approach prevents any directional bias.

The 6-km ~~radius from each grid point, and~~limitation, the Gaussian function and its standard deviation of 2 (for the kernel estimation), were tuned and chosen to: a) capture different seismic patches along active faults; b) be significantly larger than the location horizontal median error (~1.2 km; Wetzler and Kurzon, 2016); c) assign higher weight to events closer to the evaluated grid-point; d) include as many events as possible for achieving statistical significance at each of the grid-points.

The *earthquake kernel density* parameter, ρ_{Nk}, is calculated by counting all the weighted events within a 6-km radius from each grid point, dividing their sum by the sampler area (πr^2) and normalising by the duration of the earthquake catalogue:

$$\rho_{Nk} = \frac{\sum_{n=1}^{N} e^{-\frac{d(n)^2}{2\sigma^2}}}{T\pi r^2} \qquad (1)$$

where N is the total number of events within the radius r, $d(n)$ is the distance between an event n and the circle centre; σ is the standard deviation of the Gaussian function, and T is the duration of the earthquake catalogue. Units are $[events/km^2/yr]$.

The M_0 *kernel density* parameter, ρ_{M0k}, is obtained by first calculating the seismic moment released by each event separately, using the empirical relation between M_0 and M_L, as obtained by Shapira and Hofstetter (1993) after converting units from *dyne-cm* to *N-m*:

$$log[M_0] = 10 + 1.3M_L \qquad (2)$$

Secondly, each amount of energy is weighted according to the distance of the corresponding event from the circle centre (like the calculation of the *earthquake kernel density*). Then, we sum the weighted-M_0 released from all the events within a 6-km radius, divide the sum by the circle area (πr^2) and normalise by the duration of the catalogue:

$$\rho_{M0k} = \frac{\sum_{n=1}^{N} M_0(n) e^{-\frac{d(n)^2}{2\sigma^2}}}{T\pi r^2} \qquad (3)$$

where N is the total number of events within the radius r, $M_0(n)$ is the seismic moment released from an event n according to Eq. 2, *d(n)* is the distance between an event n and the circle centre, σ is the standard deviation of the Gaussian function, and T is the duration of the earthquake catalogue; units are $[joule/km^2/yr]$.

4.3 Distribution maps of the spatial processing parameters

4.3.1. Earthquake Kernel Density

The *earthquake kernel density* (Fig. 3) captures the main active tectonic sources and seismic patches, according to ~35 years of instrumental seismicity. As expected, most of the earthquakes are concentrated along the main fault zone of the DST, and to a lesser extent along the CTF, including its offshore continuation in the Mediterranean Sea. In the southwest, seismicity is observed in the area of the Gulf of Suez. Small patches appear in different spots, mainly west of the DST, raising the issue of the detectability of the network east of it. We note that the International Seismological Centre catalogue reveals large portion of events recorded east of the DST as well (Palano et al., 2013). The most prominent zone of seismicity that is not associated with known active tectonic feature is northwest of the Gulf of Elat.

A more detailed scan of the seismicity from south shows that the prominent patches of seismicity along the DST are located in the Gulf of Elat, the Arava valley, and the Dead Sea ~~Basin~~basin. Northwards, seismicity becomes more distributed, reflecting the intersection between the DST and the CTF (Fig. 1). North of the intersection, the Jordan valley segment of the DST is sparse with seismicity. However, further north, dominant seismicity patches are seen in the Sea of Galilee, and in the Hula valley. Northwest of the Hula valley, another zone of intense seismicity is captured, which might be associated with faults related to the Roum fault, west of the ~~LBR~~LRB (Meirova and Hofstetter, 2013).

4.3.2. Seismic moment kernel density

The distribution of the average annual moment density released from all earthquakes, assuming them as point sources, is shown in ~~figure~~Fig. 4. Since the amount of energy released by each earthquake differs significantly according to its magnitude, this parameter is presented on a logarithmic scale. Overall, the *Mo kernel density* distribution emphasises the seismic activity along the DST, with similarity to the *earthquake kernel density* distribution (Fig. 3). Still, the distribution is less smooth due to single events differing significantly from each other in their corresponding Mo release.

The Gulf of Elat includes the largest event recorded in the catalogue, the $\mathrm{M_W} = 7.2$ 1995 Nuweiba earthquake (Hofstetter et al., 2003), two order of magnitudes larger than the second-largest event ($\mathrm{M_d} = 5.6$), hence the significantly higher values in its vicinity. The spatial distribution of the *Mo kernel density* reveals a wide zone of deformation surrounding the gulf flanks, much wider than the relatively narrow gulf. This can be partially explained by the poorly-constrained epicentre locations, far away from the network coverage (Fig. A2). The *seismic moment kernel density* reflects strongly the most significant events that occurred in the past 35 years; among them are the $M_w = 5.1$ 2004 event in the Dead Sea (Hofstetter et al., 2008), and the $M_d = 5.3$ 1984 event associated with the CTF. In contrast with the distribution of the *earthquake kernel density*, the *Mo kernel density* does not reflect seismic swarms, unless they consist of high magnitudes. This contrast is predominant in the Sea of Galilee, which contains high *earthquake kernel density* (Fig. 3) but is less significant in the *seismic moment kernel density* (Fig. 4).

5. The main seismic sources

Figures 3 and 4 show a strip of dense seismic events and moment release along the DST and its main branches. We now combine these data with geologic, geodetic and ~~paleoseismologic~~paleo-seismologic measurements to generate the main seismic sources map, which displays regional faults that ~~demonstrates~~demonstrate slip rates inferred ~~here~~ as ≥ 0.~~5mm~~5 mm/yr during the Holocene. Tectonic and geometric characteristics (i.e~~.,~~. segment length & orientation) are also considered. We define the main seismic sources as faults that are likely to generate significant earthquakes (M ≥ 6.0), which can impact Israel (and also neighbouring countries) and constitute potential sources for different sorts of damages (i.e~~.,~~. ground ~~motion and acceleration~~shaking, landslides, liquefactions and tsunamis). These faults and their map (Fig. 5) are essential for ~~seismotectonic~~seismo-tectonic modelling of Israel, Probabilistic Seismic Hazard Analysis (PSHA) and eventually for generating ground motion maps. Below, we define two subgroups of faults divided by their tectonic characteristics and their slip rates. Off-shore inferred continuations of the main faults are also presented (dashed lines in Fig. 5).

~~5.1 Potential sources for large earthquakes~~

5.1 Main strike-slip segments of the DST

This category (solid black ~~lines~~ in ~~Fig. 5~~the map) includes ~~the main sinistral and oblique fault segments of the DST~~ potential sources for Large to Major earthquakes in the region. According to paleoseismic and/or geodetic investigations (Table ~~5~~1; Fig. A3), these faults are associated with Holocene ~~slip rates of 1 mm/yr < V_S < 5 mm/yr, where V_S is the~~ average sinistral slip ~~component accommodated by these faults~~rates of 1 – 5 mm/yr. Equally important, all the faults in this category are relatively long with a preferable slip orientation according to the present stress field (Jaeger et al., 2007~~).~~; Eyal and Reches, 1983). Our database (Fig. 5) includes fault segments from this subgroup ~~which~~that are located up to 150-km away from Israel. As noted in Sec. 4, the only recorded large earthquake, the 7.2 M_W Nuweiba ~~earthquake~~event, occurred on the Aragonese Fault and was associated with mean slip of 1.4–3 m (Baer et al., 1999).

South to Lebanon, geodetic measurements show ~ 4–5 mm/yr sinistral slip ~~(~~rate (Masson, 2015; Hamiel et al., 2016; 2018a~~; 2018b; Masson, 2015).~~, b). Faulting in Lebanon is partitioned to a few branches (Fig. ~~3~~5) and the specific rates are less constrained. While the Yammuneh and the Serghaya faults can undoubtedly be considered as independent sources for significant earthquakes, the status of the shorter, Rachaiya and Roum fault branches are less clear. Nevertheless, according to the present state of information (~~see~~ for example, Nemer and Meghraoui (2006)), we cannot rule them out and they remain part of this group.

Previous analyses of maximum earthquake magnitude based on historical earthquakes or on background seismicity predicted magnitudes of ≤ 7.8 M_w for the largest segments (e.g., Stevens and Avouac., 2017; Klinger et al., 2015; Hamiel et al., 2018a).

~~5.2. Potential sources for intermediate earthquakes~~

5.2. Main marginal faults and branches

This ~~category~~subgroup (pale blue lines in ~~Fig. 5~~the map) consists of fault zones with lengths of several ~~dozen~~to dozens kilometres that are associated with the DST~~, and display~~. Based on several previous works (Table 2), we estimated the slip rates ~~of~~along these fault zones as 0.5 ~~mm/yr ≤ V_S ≤~~ 1 mm/yr~~ (Table ~~. All the fault segments are located inside (or partly inside) the overlap zone which defined by the two seismological analyses (Fig. 6).

~~This~~The subgroup includes the Hazbaya Fault in Lebanon; the fault zone in the western and eastern margins of the Dead Sea; the marginal faults of the Hula basin; the Carmel - Tirza fault zone (CTF) and the ~~CTF~~Elat Fault (Fig. 5). The partitioning of the slip rate across parallel segments in any given fault zone is usually below the geodetic measurement (or the information) resolution. Therefore, the segments ~~of this category~~presented in Figure 5 are representative, but not necessarily the most active within a given system.

Due to the lack of reliable historical and paleo-seismological evidences, the evaluation of maximum possible magnitude on these faults is ~~usually hard~~less certain and requires several assumptions. First, we consider here a local rupture on ~~a segment~~segments from a given system and disregard a rupture of the entire system as part of an extremely large earthquake on the main strike-slip faults (~~such a rupture is discussed~~as evaluated separately in Sec. 5.1). In addition, we assume that the longest possible subsurface rupture length is similar to the length of the segment's surface trace. For example, the Carmel Fault, the northern fault in the CTF is up to 40-km length (on- and off- shore). According to some published scaling relationships, rupturing along its entire length can be associated with up to ~7 Mw earthquakes (Wells and Coppersmith, 1994; Stirling et al., 2013). However, here we assume again that such magnitudes must be interconnected with an earthquake along a much larger DST segment~~,~~ (Agnon, 2014), and not confined to a local ~~fault (Agnon, 2014).~~ segment. We therefore assume a maximum rupture length of ~10–20 km along faults from this subgroup and correspondingly to maximum magnitudes of ~~6.0 <~~ $M_w < 6.5$ (Wells and Coppersmith, 1994). ~~The~~ We note that the data on the Elat Fault is based only on ~~evidence~~evidences from its northern edge (e.g. a catastrophic event at 2.3ka inferred by Shaked et al. (2004)), while the rates at its offshore parts are less constrained. ~~Shaked et al. (2004) inferred a catastrophic event at 2.3ka~~ Further work on ~~the Elat Fault.~~its subsurface section and the connection to the main sinistral displacement is required for better evaluation of its seismic potential.

~~Large~~We additionally note that large earthquakes along the Cyprian Arc (Fig. 1) can also generate tsunamis that might affect the coastline of Israel (Salamon et al., ~~2000~~2007). This source is not analysed and mapped here, but should be taken into account in regional ~~seismotectonic~~seismo-tectonic models.

6. Capable faults

6.1 Framework and principles

The hazard of surface rupture is defined as the likelihood of an earthquake that will rupture the surface within a certain time window. This likelihood is based on knowledge about the past and present fault kinematics and dynamics. The determination of the relevant time reference for young faulting is usually dictated by different constrains and applications. In the United States, faults are commonly considered to be active for planning constructions if they have ruptured the surface at least once in the past 10ka. However, regional conditions, such as sedimentary cover or available age dating of pertinent geological units can affect this determination. For example, faults that are defined as “Active” in the “Design Provisions for Earthquake Resistance of Structures” in Israel are those that ruptured the surface in the past 13ka (Heimann, 2002). This is the age of the top of the lake formation that covers significant parts of the Dead Sea valleys.

The time reference for special constructions such as dams and nuclear power plants is usually much longer, because the possible damage to the construction has severe regional implications. According to the International Atomic Energy Agency (IAEA) Safety Fundamentals (IAEA, 2010), capable faults are these with evidence for displacement since thousands or millions of years, depending on how tectonically active is the ~~region activity~~area. Here, the Quaternary period is selected as the time reference for sensitive facilities due to two main reasons: a) we assume that faults that were active during the present regional stress regime (Zoback, 1992) are more likely to activate in the near future. The regional stress state within the Quaternary period ~~is~~ represents well the current stress field (Eyal and Reches, 1983; Hofstetter et al., 2007; Garfunkel, 2011; Palano et al., 2013). We note that "regional stress field" (Zoback, 1992) as a criterion for active faulting is closely related to the "tectonic regime" suggested by Galadini (2012). b) Quaternary geological units are mostly well defined in the region.

The primary and secondary criteria for sorting the faults are listed in a descending order of categorisation, meaning that faults are initially examined according to the first criterion, and only if they do not match it, they are examined according to the second criterion, and so on.

~~Finally, in regions where Quaternary cover is~~Where geological evidences are absent, we utilise a seismological criterion (Fig. 6), ~~based on~~under the assumption that faults ~~that are~~ associated with seismically active subzones are more likely to have ruptured the surface in the Quaternary compared to others.

Finally, because of the limitation of our database, mapped capable faults (Fig. 7) are limited to Israel region, unless their continuations spread to the neighbouring countries.

6.2 Primary criteria

1. Main strike-slip faults of the DST: identified here as main sources for large regional earthquakes (Fig. 7).
2. **2.** Faults with direct evidence of Quaternary activity: faults that have been mapped offsetting Quaternary formations or that have been interpreted by scientific

publications (Table A2) to rupture the earth's surface at least once since the Quaternary. This criterion is mainly related to zones covered by Quaternary units.

6.3 Secondary criteria

Faults that have no field relationship with Quaternary formations consequently show no direct evidence for Quaternary faulting. We therefore designed the next criteria under the rationale that they expand the database with faults that reasonably have been active since the Quaternary, based on the following ~~three sub-~~criteria:

1. First order branches and the marginal faults of the DST

   a) First order branches of faults that are mapped following the primary criteria. A fault branch is defined here as splitting at an acute angle from another fault. The throw direction of the fault and its branches are also taken into account.
   b) Faults that bound the DST basins, separating Quaternary formations from older rocks and are associated with a sharp topographic boundary of at least 100 meters.
   c) Faults that emerge from Quaternary sediments that infill the DST valleys and are likely to branch off ~~of~~ the main DST segments.

2. Faults associated with recent seismicity

   ~~it~~It is challenging to match the faults and recent seismicity and assume they ruptured the surface at least once since the beginning of the Quaternary, because there are thousands of mapped faults, the high-resolution geophysical data about ~~the~~ fault structures in depth are scarce, and the hypocentres' location uncertainties are large. In order to define the seismicity-based criterion, we create polygons for each of the parameters. The polygons are defined by ~~a~~ threshold ~~value~~values, so that each of them is the smallest to cover continuously the whole length of the most active tectonic feature in the region~~, continuously in~~. In our case study, this ~~case,~~feature is the DST~~;~~ ~~excluding~~, but we exclude the relatively silent northern section of the Jordan Valley segment (I in Fig. 6). Therefore, the overlap area (Fig. 6) of the two polygons consists of at least the minimum level of both *seismic moment kernel density* and *earthquake* *kernel density*, along the DST in the Israel region. Hence, if a fault is within the overlap area, it means that it is associated with at least a minimum level of seismicity along the most active tectonic feature, and thus it is likely to be seismogenic. We further assume a relation between a fault mapped surface trace and a possible past surface rupture, ~~in order to select~~for selecting the most prominent faults. Considering scaling relations between fault dimensions and source parameters, faults that contain surface traces of at least 6-km (corresponding to $M_W \geq 6.0$ earthquakes; Wells and Coppersmith, 1994; Stirling et al., 2002; Mai and Beroza, 2000) within the 'overlap area' are assumed here as Quaternary faults.

3. Subsurface faults

Subsurface and offshore continuation of the main DST strike-slip segments, and a few other faults with published details for both their subsurface extension and their Quaternary activity are marked (the majority are in Fig. 5). In addition, we map other faults that offset dated Quaternary units, with well-constrained near-surface location inferred from high-resolution seismic data. We exclude subsurface faults when their exact location and activity period are less constrained. Fault segments that were mapped as concealed (mostly by thin alluvium) in the 1:50,000 maps and are the continuation of Quaternary faults are marked as ordinary surface traces.

7. Discussion

7.1 Methodological aspects and applications for hazard evaluations

Regions with intermediate seismicity rates present a challenge for hazard evaluation; ~~while~~whilst the hazard ~~is~~might be perceptible, the seismic data ~~is~~ and the geological evidences for recent surface rupture are sparse comparing to very active zones. ~~Taking into the account~~Considering that the earthquake phenomenon is a stochastic process and its predictability is limited, we develop a methodology ~~that takes~~for mapping and characterising hazardous faults, by taking advantage of incorporating interdisciplinary information with statistical seismological analyses~~ for seismic hazard evaluation. We delineate~~.

Two regional fault maps are presented; one is relevant for regional ground shaking models (Fig. 5), and the other for surface rupture nearby facilities that are particularly vulnerable to this hazard (Fig. 7). In addition to the approach of classifying faults by the recency of faulting or by their recurrence intervals (Machette, 2000 and references therein), we utilise other criteria such as seismological patterns (Sec. 4) and tectonic configuration (Sec. 6.3). In particular, we use the distribution of the *earthquake kernel density* ~~of earthquakes~~ and ~~of~~ the *seismic moment* ~~release by analysing recorded seismicity and applying statistic-based data processing (Figs. 3, 4).~~ *kernel density* to test the relevancy of faults for different hazards. Fig. A4 reveals that most of the capable faults, which are mapped based on the geological criteria, could have entered the map also by the seismological criterion (ignoring its 6-km fault length limitation). The match between the geological-categorised faults and the area defined by the seismological analysis reinforces the methodological concept of utilising the two seismological distributions that are, to a large extent, independent of one another. Moreover, faults that are defined here as ‘main seismic sources’ according to specific tectonic conditions (i.e. slip rate, geometry, structure) are well correlated with the zone defined by our seismological analysis (Fig. 6). This emphasises the significance of this analysis, especially when slip rates are slow or under debate (as in Sec. 5.2).

The internal hierarchic categorisation of faults in both maps (Figs. 5, 7) enables separating different fault groups, and can later be implemented if a specific hazard is considered or if risk evaluation is applied. However, ~~instrumental seismological data is practically limited, and the precision of the results depends on the amount and the quality of the data, regardless of the specific statistical method. This gap is closed by geodetic measurements, paleo-seismology and historical information.~~

~~Throughout the capable fault map (Fig. 7), the information about the seismic intervals of most of the faults is poor compared with these of the DST main strike-slip faults. Faults of different categories are distributed in the same areas: these that show direct evidence of Quaternary faulting, and those that fit seismo-tectonic criteria. For example, branches of the DST main segments that do not cross Quaternary sediments, are marked based on tectonic rationale. Moreover,~~ we note that although faults are marked by hierarchical criteria, the different categories are in many cases ~~the different categories~~ complement each other rather than show hierarchy of the activity level. ~~Accordingly, the distribution of the~~

~~different faults is rather homogeneous throughout the map (Fig. 7). This includes faults marked based on the seismicity-based criterion. The Quaternary faults are superimposed on the seismicity polygons of this criterion (Fig. A3) and reveal that many the majority of the faults, which are mapped based on the geological criteria, could have enter the map also by the seismological criterion (ignoring its 6-km fault length limitation). Thus, the correlation between the recorded~~The grid-based distributions of the obtained seismicity parameters are utilised here together with fault geometry parameters (length and orientation) for defining capable faults. The advantage of this integration is expressed where the seismological criterion (Sec. 6. 3) defines capable faults in zones where young formations are scarce (Fig. 7). Just as important, our database of gridded seismicity, with possible adjustments, can be implemented as an independent source for hazard evaluations, and as a complementary to the regional databases of mapped faults in zones of subsurface faults.

Although our methodology is demonstrated for the Israel region, the approach is universal, and is particularly useful in domains of intermediate seismicity rates or limited field evidences. The criteria, when implemented in other regions, should be adjusted according to the regional and local seismo-tectonic settings. For example, our seismicity ~~and the Quaternary faults support the design~~-based analysis is not considering the orientation and the inclination of the ~~seismicity-based criterion. On the other hand, we do~~fault surface when epicentre locations and fault traces are correlated together, because most of the faults in Israel region are characterised by steep dips. This cannot be neglected in low-angle fault zones or convergence regime. Finally, our approach of hierarchic tectonic criteria for categorising faults can be applied in principle also when local siting of an infrastructure is considered. However, faults with extremely long recurrence intervals, located along zones that are not ~~define~~covered by young formations might be difficult to detected, even when seismo-tectonic criteria are considered. Moreover, faults that constitute a mechanical potential for slip ~~(for example,~~, such as conjugate fault sets~~) as capable~~ (Eyal and Reches, 1983) or old faults that can be reactivated by stress triggering (Stein et al., 1997) are not defined as capable in our regional analysis, unless further geological or seismological evidence for Quaternary activity ~~is existed. Such a mechanical criterion, however, should be considered and re-evaluated during the specific siting~~

~~stage~~exists. Therefore, local siting, in particular of sensitive infrastructure, might require stricter criteria both for surface rupture and ground shaking, depending on the specific requirements.

~~While~~

7.2 Implications for local tectonics and slip dynamics

The DST accommodates most of the seismic activity~~ follows the DST, some areas along it are associated with~~, but also contains zones of very sparse seismicity (Fig. ~~6).~~6). The seismicity distribution maps (Figs. 3, 4) exhibit enhanced seismicity in the pull-apart basins and reduced activity in the long straight segments. The heterogeneous distribution can be explained by the tendency of stress amplification and failure to concentrate locally within zones of geometric irregularity, such as releasing bends (e.g. Segall and Pollard, 1980; Reches, 1987), whereas the long segments can accommodate higher stresses that are released in single earthquakes of more seismic moment release (Sagy and Lyakhovsky, 2019). At the northern section of the Jordan Valley long segment, section I is the least active part of the DST during the last ~35 years. ~~Geodetic analysis demonstrates that this section creeps~~Shallow crust creep along the northern part of this segment at a rate of approximately half ~~of~~ the total plate motion (Hamiel et al., 2016~~). This creep, together with~~) and potential partitioning of the DST activity to the CTF~~,~~ (Sadeh et al., 2012; Hamiel et al., 2018b) might ~~cause~~reduce the ~~relative reduction of earthquakes~~seismicity rate in section I (Fig. 6). Sections II and III, at the middle and the northern sections of the Arava segment, are also associated with sparse seismicity, but to a lesser extent. With no indication for creep, the reduction of seismicity might be attributed to local locking of the main fault~~ or to the influence of other structures~~. Structural and lithological contrasts in fault junctions (e.g. ~~WSW-ENE orientated~~the SNB and ~NNE striking faults~~ of the Sinai-Negev shear belt (Bartov, 1974)). Further research of these zones is required for better understanding the ~~) might also affect increasing or decreasing of local ~~variation of~~seismicity along the ~~seismic patterns.~~segments.

Figures 3 and 4 point on a ~SE-NW trending seismological lineament with intensified seismicity in its southeast (IV in Fig. 6, referred here as East Sinai zone). This lineament seems to branch off the DST in a zone of a structural boundary, between the deep tectonic basins of the Gulf of Elat (Ben-Avraham, 1985) and the Arava valley, a "structural and topographic saddle with hardly any "rift-valley" in its centre" (Garfunkel, 1981). Since the seismic activity implies that it may run further northwest, we refer to it as the Elat – Bardawil Lineament (EBL). Its orientation, sub-parallel to the CTF, the Suez rift and the Red Sea spreading centre, might indicate on a similar extensional feature (see Fig. A5). This possibility is supported by geodetic analysis (Palano et al., 2013), a focal mechanism solution within this zone (Abdelazim et al., 2016), and by the orientation of nearby Quaternary faults (Fig. 6) and other fault traces in Sinai, outside our high-resolution data (e.g. Eyal et al., 1980). However, currently there are no available high-resolution maps to confirm the existence of faults associated with the seismicity in the East Sinai zone. We interpret the seismicity within the EBL as related to reactivation of subsurface faults that were either formed during the post-Eocene Red Sea rifting or even older faults. Further research is required for better characterisation of this activity and its relationship to the regional tectonics.

Finally, relatively long E-W trending faults (SNB) cross the south of Israel and Sinai and some of them are marked as Quaternary faults (Fig. 7, Fig. A4). However, there are no geologic or geodetic indications for any activity along them since the early Pleistocene, and the associated seismic activity mostly concentrates in their junctions with the DST. We therefore assume that these dextral oblique slip faults are inactive in the present regional stress field, and their reactivation may generally decrease with increasing distance from the DST.

8. Conclusions

1. Mapping and characterising faults that pose seismic hazard, particularly in regions with intermediate seismicity rates and/or where young formations are sparse, require ~~generating~~developing an interdisciplinary regional database and ~~developing~~ hierarchical seismo-tectonic criteria. With respect to the specific dictated requirements, faults that are potential sources for the far-field and for the near-field (i.e., surface rupture) hazards should be analysed by different criteria; both represent seismic hazard of significant earthquakes, but within different time frames.

~~2. The regional main seismic sources are primarily defined by the recent slip rates. Geologic and geodetic slip rates, as well as long historical record and high-resolution mapping enable reliable definition of faults that are likely to generate large earthquakes. All the main seismic sources in the Israel region (Fig. 5) are related to the DST activity.~~

~~3. The time~~2. We design a seismicity-based criterion that utilises the distribution of two parameters: the *earthquake kernel density* and the *seismic moment kernel density*. The success of this selection is demonstrated by the match between the geological-categorised faults and the seismicity criterion (Fig. A4). The union zone defined by these two statistical distributions is efficient in both definition of the main seismic sources (Fig. 6) and in categorising capable faults (Fig. 7).

3. The hierarchic seismo-tectonic criteria ideally reflects the degree of certainty for recent faulting, and can later be implemented if a specific hazard is considered or if risk evaluation is applied.

4. The temporal reference for local planning of ~~special constructions~~critical facilities such as dams and nuclear power plants is usually long, because the possible damage to the construction has severe regional implications. We ~~selected~~select the Quaternary period as the relevant time frame for capable faults in the region of Israel. While this time frame (2.6 Ma) is longer than the previous for defining capable faults for a potential local nuclear power plant (IEC and WLA, 2002), it is justified by considering the regional stress field, the regional stratigraphic configurations and the criteria that focus on surface rupture rather than general fault movements. We ~~conclude~~suggest that tectonic and stratigraphic conditions, as well as the accessibility of geologic maps and their resolutions, should be ~~taken into account~~considered for defining the time frame for capable faults.

~~4. We design a seismicity-based criterion that is based on the distribution of two parameters: the *Earthquake Kernel Density* and the *Seismic Moment Kernel Density*. The success of this selection is further reinforced by the match between the geological-categorised faults and the seismicity criterion (Fig. A3).~~

5. Beyond planning of special constructions, the developed database and the maps that are generated and presented here constitute further applications for planning and research. The regional main seismic sources map (Fig. 5) is fundamental for seismotectonic

modelling and eventually for generating ground motion prediction maps (e.g. by PSHA) that ~~include~~are essential ~~information~~ for construction planning~~, such as peak ground acceleration~~. The capable fault database and the related maps (Figs. 2-4, 6-7) lay the foundation for further study of the regional Quaternary faulting and tectonics in the Israel region. Furthermore, the methodology, which is based on categorisation and sub-categorisation by seismo-tectonic hierarchic criteria, enables differentiation of hazard potential and can be applied in other regions around the world.

6. The relation between instrumental seismicity, geodetic slip rates and the internal structure of the main fault zone enables revealing seismo-tectonic patterns in an investigated region. Specifically, we recognise along the DST zones of enhanced or reduced seismicity, which can be controlled by slip partitioning, creep, geometric irregularities associated with releasing bends, and litho-structural complexities in fault junctions. In addition, we identify a zone of seismicity that seems to diverge from the main fault zone towards ~NW (EBL in Fig. A5; Fig. 6). Its orientation and a few independent evidences imply that it reflects extension-related activity, accommodated by (subsurface?) fault system that branch off the DST.

Acknowledgments

We thank the following people for their ~~collaboration and~~ assistance: R. Amit, Y. Avni, Y. Bartov, Z. Ben-Avraham, G. Baer, M. Beyth, A. Borshevsky, R. Calvo, Y. Eyal, Z. Garfunkel, H. Ginat, Z. Gvirtzman, Y. Hamiel, S. Hoyland, S. Ilani, R. Kamai, W. Lettis, T. Levi, D. Mor, C. Netzer, P. Nuriel, Y. Sagy, A. Salomon, A. Sneh, R. Weinberger, E. Zilberman. We also thank three anonymous reviewers for their constructive and important comments.

9. References

Abdelazim, M., Samir, A., El-Nader, I. A., Badawy, A., Hussein, H.: Seismicity and focal mechanisms of earthquakes in Egypt from 2004 to 2011, NRIAG Journal of Astronomy and Geophysics, 5(2), 393–402, 2016.

Agnon, A.: Pre-instrumental earthquakes along the Dead Sea Rift, in: Dead Sea Transform Fault System: Reviews, edited by: Garfunkel, Z., Ben-Avraham, Z., and Kagan, E. J., Springer, Dordrecht, the Netherlands, 207–262, 2014.

Aldersons, F., Ben-Avraham, Z., Hofstetter, A., Kissling, E., and Al-Yazjeen, T.: Lower-crustal strength under the Dead Sea basin from local earthquake data and rheological modeling, Earth Planet. Sc. Lett., 214, 129–142, 2003.

Ambraseys, N.: Earthquakes in the Mediterranean and Middle East: a multidisciplinary study of seismicity up to 1900, Cambridge University Press, New York, 2009.

Amit, R., Zilberman, E., Enzel, Y. and Porat, N.: Paleoseismic evidence for time dependency of seismic response on a fault system in the southern Arava Valley, Dead Sea rift, Israel, Geol. Soc. Am. Bull., 114(2), 192–206, 2002.

Atkinson, G. M., and Goda, K.: Probabilistic seismic hazard analysis of civil infrastructure, in: Handbook of Seismic Risk Analysis and Management of Civil Infrastructure Systems, edited by: Tesfamariam, S., and Goda, K., 3–28, https://doi.org/10.1533/9780857098986.1.3, 2013.

Ben-Avraham, Z.: Structural framework of the Gulf of Elat (Aqaba), Northern Red Sea, J. Geophys. Res., 90(B1), 703–726, 1985.

Baer, G., Sandwell, D., Williams, S., Bock, Y. and Shamir, G.: Coseismic deformation associated with the November 1995, Mw= 7.1 Nuweiba earthquake, Gulf of Elat (Aqaba), detected by synthetic aperture radar interferometry, J. Geophys. Res.: Solid Earth, 104(B11), 25221–25232, 1999.

Bartov, Y.: A Structural and paleogeographical study of the central Sinai faults and domes, Ph.D. thesis, Hebrew University of Jerusalem, 143 pp. (in Hebrew, English abstract), 1974.

Bartov, Y., and Sagy, A.: Late Pleistocene extension and strike-slip in the Dead Sea Basin, Geol. Mag., 141(5), 565–572, 2004.

Bentor, Y. K., and Vroman, A.: A Structural contour map of Israel (1:250,000) with remarks on its dynamic interpretation, Bull. Res. Counc. Isr., 4(2), 125–135, 1954.

Calvo, R., and Bartov, Y.: Hazeva Group, southern Israel: New observations, and their implications for its stratigraphy, paleogeography, and tectono-sedimentary regime, Israel. J. Earth Sci., 50, 71-99, 2001.

Ellenblum, R., Marco, S., Kool, R., Davidovitch, U., Porat, R., and Agnon, A.: Archaeological record of earthquake ruptures in Tell Ateret, the Dead Sea Fault, Tectonics, 34, 2105–2117, https://doi:10.1002/2014TC003815, 2015.

Eyal, Y., and Reches, Z.: Tectonic analysis of the Dead Sea Rift Region since the Late-Cretaceous based on mesostructures, Tectonics, 2(2), 167–185, 1983.

Eyal, M., Bartov, Y., Shimron, A. E., Bentor, Y. K., 1980. Sinai – Geological Map: scale 1:500,000. Tel Aviv: Survey of Israel.

Ferry, M., Meghraoui, M., Karaki, N. A., Al-Taj, M., Amoush, H., Al-Dhaisat, S., and Barjous, M.: A 48-kyr-long slip rate history for the Jordan Valley segment of the Dead Sea Fault, Earth Planet. Sc. Lett., 260, 394–406, 2007.

Ferry, M., Meghraoui, M., Abou Karaki, N., Al-Taj, M., and Khalil, L.: Episodic Behavior of the Jordan Valley Section of the Dead Sea Fault Inferred from a 14-ka-Long Integrated Catalog of Large Earthquakes, B. Seismol. Soc. Am., 101(1), 39–67, https://doi:10.1785/0120100097, 2011.

Galadini, F., Falcucci, E., Galli, P., Giaccio, B., Gori, S., Messina, P., Moro, M., Saroli, M., Scardia, G. and Sposato, A.: Time intervals to assess active and capable faults for engineering practices in Italy, Eng. Geol., 139, 50–65, 2012.

Garfunkel, Z.: Internal structure of the Dead Sea leaky transform (rift) in relation to plate kinematics, in: The Dead Sea Rift, edited by: Freund, R., Garfunkel, Z., Tectonophysics, 80, 81–108, 1981.

Garfunkel, Z.: Constrains on the origin and history of the Eastern Mediterranean basin, Tectonophysics, 298, 5–35, 1998.

Garfunkel, Z.: The long- and short-term lateral slip and seismicity along the Dead Sea Transform: An interim evaluation, Israel J. Earth. Sci., 58(3), 217–235, https://doi.org/10.1560/IJES.58.3-4.217, 2011.

Garfunkel, Z.: Lateral motion and deformation along the Dead Sea transform, in: Dead Sea Transform Fault System: Reviews, edited by: Garfunkel, Z., Ben-Avraham, Z., and Kagan, E. J., Springer, Dordrecht, the Netherlands, 109–150, 2014.

Garfunkel, Z., and Bartov, Y.: The tectonics of the Suez rift, Geological Survey of Israel Bulletin, 71, 1–44, 1977.

Garfunkel, Z., and Ben-Avraham., Z.: Basins along the Dead Sea transform, Mémoires du Muséum national d'histoire naturelle, 186, 607–627, 2001.

Gibbard, P. L., Head, M. J., Walker, M. J. and Subcommission on Quaternary Stratigraphy, Formal ratification of the Quaternary System/Period and the Pleistocene Series/Epoch with a base at 2.58 Ma, J. Quaternary Sci., 25(2), 96–102, 2010.

Gomez, F., Meghraoui, M., Darkal, A. B., Hijazi, F., Mouty, M., Suleiman, Y., Sbeinati, R., Darawcheh, R., Al-Ghazzi, R., and Barazabgi, M.: Holocene faulting and earthquake recurrence along the Serghaya branch of the Dead Sea Fault system in Syria and Lebanon, Geophys. J. Int., 153, 658–674, 2003.

Gomez, F., Karam, G., Khawlie, M., McClusky, S., Vernant, P., Reilinger, R., R., Jaafar, R., Tabet, C., Khair, K., and Barazangi, M.: Global Positioning System measurements of strain accumulation and slip transfer through the restraining bend along the Dead Sea fault system in Lebanon, Geophys. J. Int., 168(3), 1021–1028, 2007.

Hamiel, Y., Piatibratova, O., and Mizrahi, Y.: Creep along the northern Jordan Valley section of the Dead Sea Fault, Geophys. Res. Lett., 43(6), 2494‑2501, 2016.

Hamiel, Y., Masson, F., Piatibratova, O., and Mizrahi, Y.: GPS measurements of crustal deformation across the southern Arava Valley section of the Dead Sea Fault and implications to regional seismic hazard assessment, Tectonophysics, 724–725, 171–178, https://doi.org/10.1016/j.tecto.2018.01.016, 2018a.

Hamiel, Y., Piatibratova, O., Mizrahi, Y., Nahmias, Y., and Sagy, A.: Crustal deformation across the Jericho Valley section of the Dead Sea Fault as resolved by detailed field and geodetic observations, Geophys. Res. Lett., 45, 3043‑3050, https://doi.org/10.1002/2018GL077547, 2018b.

Heimann, A.: Active faulting in Israel, Geologiacl Survey of Israel Report No. GSI/07/02, Jerusalem, 33 pp. (in Hebrew), 2002.

Hofstetter, A., van Eck, T., and Shapira, A.: Seismic activity along fault branches of the Dead Sea-Jordan transform system: the Carmel – Tirza fault system, Tectonophysics, 267, 317‑330, 1996.

Hofstetter, A., Thio, H. K., and Shamir, G.: Source mechanism of the 22/11/1995 Gulf of Aqaba earthquake and its aftershock sequence, J. Seismol., 7, 99‑114, 2003.

Hofstetter, R., Klinger, Y., Amrat, A.-Q., Rivera, L., and Dorbath, L.: Stress tensor and focal mechanisms along the Dead Sea fault and related structural elements based on seismological data, Tectonophysics, 429, 165–181, 2007.

Hofstetter, R., Gitterman, Y., Pinsky, V., Kraeva, N., and Feldman, L.: Seismological observations of the northern Dead Sea basin earthquake on 11 February 2004 and its associated activity, ~~Isr~~Israel. J. Earth Sci., 57, 101–124, 2008.

International Atomic Energy Agency (IAEA): Seismic ~~Hazards~~hazards in ~~Site Evaluation~~site evaluation for ~~Nuclear Installations Specific Safety Guide~~nuclear installations specific safety guide: IAEA Safety Standards Series No. SSG-9, International Atomic Energy Agency, Vienna, 2010.

IEC and WLA (Israel Electric Corporation and William Lettis & Associates, Inc.): Shivta-Rogem Site Report. Israel Electric Corporation, Ltd., 2002.

Jaeger, J. C., Cook, N. G. W., and Zimmerman, R. W.: Fundamentals of Rock Mechanics (4th ed.), Blackwell, Malden, Mass., 488 pp., 2007.

Joffe, S., and Garfunkel, Z.: Plate kinematics of the circum Red Sea – a re-evaluation, in: Sedimentary ~~Basins~~basins within the Dead Sea and ~~Other Rift Zones~~other rift zones, edited by: Ben-Avraham, Z., Tectonophysics, 141, 5-22, 1987.

Klinger, Y., Le Béon, M. and Al-Qaryouti, M.: 5000 yr of paleoseismicity along the southern Dead Sea fault, Geophys. J. Int., 202(1), ~~pp.~~313–327, 2015.

Le Béon, M., Klinger, Y., Al-Qaryouti, M., Mériaux, A. S., Finkel, R. C., Elias, A., Mayyas, O., Ryerson, F. J. and Tapponnier, P.: Early Holocene and Late Pleistocene slip rates of the southern Dead Sea Fault determined from 10Be cosmogenic dating of offset alluvial deposits, J. Geophys. Res.: Solid Earth, 115(B11), 2010.

Machette, M. N.: Active, capable, and potentially active faults—a paleoseismic perspective, J. Geodyn., 29, 387–392, 2000.

Mai, M., and Beroza, G. C.: Source scaling properties from finite-fault-rupture models~~.~~, B. Seismol. Soc. Am., 90(3), 604–615, 2000.

Marano, K. D., Wald, D. J., and Allen, T. I.: Global earthquake casualties due to secondary effects: a quantitative analysis for improving rapid loss analyses, Nat. Hazards, 52, 319–328, 2010.

Marco, S., Rockwell, T. K., Heimann, A., Frieslander, U., and Agnon, A.: Late Holocene activity of the Dead Sea transform revealed in 3D palaeoseismic trenches on the Jordan Gorge Segment, Earth Planet. Sc. Lett., 234, 189–205, 2005.

Marco, S.: Recognition of earthquake-related damage in archaeological sites: Examples from the Dead Sea fault zone, Tectonophysics, 453(1–4), 148–156, 2008.

Marco, S., and Klinger, Y.: Review of on-fault palaeoseismic studies along the Dead Sea fault, in: Dead Sea Transform Fault System: Reviews, edited by: Garfunkel, Z., Ben-Avraham, Z., and Kagan, E. J., Springer, Dordrecht, the Netherlands, 183–205, 2014.

Masson, F., Hamiel, Y., Agnon, A., Klinger, Y., and Deprez, A.: Variable behavior of the Dead Sea Fault along the southern Arava segment from GPS measurements, C. R. Geosci., 347, 161–169, 2015.

McKenzie, D. P.: Plate tectonics of the Mediterranean Region, Nature, 226, 239–243, 1970.

Meghraoui, M., Gomez, F., Sbeinati, R., Van der Woerd, J., Mouty, M., Darkal, A. N., Radwan, Y., Layyous, I., Al Najjar, H., Darawcheh, R., Hijazi, F., Al-Ghazzi, R., and Barazangi, M.: Evidence for 830 years of seismic quiescence from palaeoseismology, archaeoseismology and historical seismicity along the Dead Sea fault in Syria, Earth Planet. Sc. Lett., 210, 35–52, 2003.

Meirova, T., and Hofstetter, A.: Observations of seismic activity in Southern Lebanon, J. Seismol., 17(2), 629–644, 2013.

Neev, D., Almagor, G., Arad, A., Ginzburg, A., and Hall, J. K.: The geology of the southeastern Mediterranean Sea, Geological Survey of Israel Bulletin, 68, 1–51, 1976.

Nemer, T., and Meghraoui, M.: Evidence of coseismic ruptures along the Roum fault (Lebanon): a possible source for the AD 1837 earthquake, J. Struct. Geol., 28, 1483–1495, 2006.

Palano, M., Imprescia, P., and Gresta, S.: Current stress and strain-rate fields across the Dead Sea Fault System: Constraints from seismological data and GPS observations, Earth Planet. Sc. Lett., 369, 305–316, 2013.

Picard, L.: The geological evolution of the Quaternary in the central-northern Jordan Graben, Israel, Geol. S. Am. S., 84, 337–366, 1965.

Porat, N., Wintle, A.G., Amit, R., and Enzel, Y.: Late Quaternary earthquake chronology from luminescence dating of colluvial and alluvial deposits of the Arava valley, Israel, Quaternary Res., 46, 107–117, 1996.

Quennell, A. M.: Tectonics of the Dead Sea rift, in: Int. Geol. Congr., 20th, Mexico: Assoc. Serv. Geol. Afr., 385–405, 1959.

Reches, Z. E.: Mechanical aspects of pull-apart basins and push-up swells with applications to the Dead Sea transform, in: Sedimentary basins within the Dead Sea and other rift zones, edited by: Ben-Avraham, Z., Tectonophysics, 141, 75–88, 1987.

Reilinger, R., McClusky, S., Vernant, P., Lawrence, S., Ergintav, S., Cakmak, R., Ozener, H., Kadirov, F., Guliev, I., Stepanyan, R., Nadariya, M., Habubia, G., Mahmoud, S., Sakr, K., ArRajehi A., Paradissis, D., Al-Aydrus, A., Prilepin, M., Guseva T., Evren, E., Dmitrotsa, A., Filikov, S. V., Gomez, F., Al-Ghazzi, R., and Karam, G.: GPS constraints on continental deformation in the Africa-Arabia-Eurasia continental collision zone and implications for the dynamics of plate interactions, J. Geophys. Res.: Solid Earth, 111(B5), 2006.

Ron, H. and Eyal, Y.: Intraplate deformation by block rotation and mesostructures along the Dead Sea transform, northern Israel, Tectonics, 4(1), 85–105, 1985.

Sadeh, M., Hamiel, Y., Ziv, A., Bock, Y., Fang, P., and Wdowinski, S.: Crustal deformation along the Dead Sea Transform and the Carmel Fault inferred from 12 years of GPS measurements, J. Geophys. Res., 117, B08410, doi:10.1029/2012JB009241, 2012.

Sagy, A. and Lyakhovsky, V.: Stress patterns and failure around rough interlocked fault surface. J. Geophys. Res.: Solid Earth, 124, https://doi.org/10.1029/2018JB017006, 2019.

Sagy, A., Reches, Z. E. and Agnon, A.: Hierarchic three-dimensional structure and slip partitioning in the western Dead Sea pull-apart, Tectonics, 22(1), 2003.

Sagy, A., Sneh, A., Rosensaft, M., and Bartov, Y.: Map of 'active' and 'potentially active' faults that rupture the surface in Israel: Updates 2013 for Israel Standard 413, Geological Survey of Israel Report No. GSI/02/2013, Jerusalem, 17 pp. (in Hebrew, English abstract), 2013.

~~Sagy, A., Wieler, N., Avni, Y., Rosensaft, M., and Amit, R.: Map of active and potentially active faults that rupture the surface in Israel: Updates 2017 for Israel Standard 413, Geological Survey of Israel Report No. GSI/13/2017, Jerusalem, 19 pp. (in Hebrew, English abstract), 2017.~~

Salamon, A., Rockwell, T., Ward, S. N., Guidoboni, E. and Comastri, A.: Tsunami hazard evaluation of the eastern Mediterranean: historical analysis and selected ~~modelling~~modeling, B. Seismol. Soc. Am., 97(3), 705–724, 2007.

Schattner, U., and Weinberger, R.: A mid-Pleistocene deformation transition in the Hula basin, northern Israel: Implications for the tectonic evolution of the Dead Sea Fault, Geochem. Geophy. Geosy., 9(7), Q07009, doi: 10.1029/2007GC001937, 2008.

Segall, P. and Pollard, D. D.: Mechanics of discontinuous faults, J. Geophys. Res: Solid Earth, 85(B8), 4337–4350, 1980.

Shaked, Y., Agnon, A., Lazar, B., Marco, S., Avner, U., and Stein, M.: Large earthquakes kill coral reefs at the north-west Gulf of Aqaba, Terra Nova, 16(3), 133–138, 2004.

Shalev, E., Lyakhovsky, V., Yechieli, Y.: Is advective heat transport significant at the Dead Sea basin?, Geofluids, 7, 292–300, 2007.

Shalev, E., Lyakhovsky, V., Weinstein, Y., and Ben-Avraham, Z.: The thermal structure of Israel and the Dead Sea Fault, Tectonophysics, 602, 69–77, 2013.

Shapira, A., and Hofstetter, A.: Source parameters and scaling relationships of earthquakes in Israel, Tectonophysics, 217, 217–226, 1993.

Sneh, A., Bartov, Y., Weissbrod, T., and Rosensaft, M.: Geological Map of Israel, 1:200,000 (4 sheets), Geological Survey of Israel, Jerusalem, 1998.

Steckler, M. S., Berthelot, F., Lyberis, N., and Le Pichon, X.: Subsidence in the Gulf of Suez: implications for rifting and plate kinematics, Tectonophysics, 153, 249–270, 1988.

Stein, R. S., Barka, A. A. and Dieterich, J. H.: Progressive failure on the North Anatolian fault since 1939 by earthquake stress triggering, Geophys. J. Int., 128(3), 594–604, 1997.

Stevens, V.L. and Avouac, J.P.: Determination of Mmax from background seismicity and moment conservation, B. Seismol. Soc. Am., 107(6), 2578–2596. 2017.

Stirling, M., Rhoades, D., and Berryman, K.: Comparison of Earthquake Scaling Relations Derived from Data of the Instrumental and Preinstrumental Era, B. Seismol. Soc. Am., 92(2), 812–830, 2002.

Stirling, M., Goded, T., Berryman, K. and Litchfield, N.: Selection of earthquake scaling relationships for seismic-hazard analysis. B. Seismol. Soc. Am., 103(6), 2993-3011, 2013.

ten Brink, U. S., and Flores, C. H.: Geometry and subsidence history of the Dead Sea basin: A case for fluid induced mid-crustal shear zone? J. Geophys. Res., 117, B01406, doi:10.1029/2011JB008711, 2012.

Torfstein, A., Haase-Schramm, A., Waldmann, N., Kolodny, Y., and Stein, M.: U-series and oxygen isotope chronology of the mid-Pleistocene Lake Amora (Dead Sea basin), Geochim. Cosmochim. Ac., 73(9), 2603–2630, 2009.

Wells, D. L., and Coppersmith, K. J.: New empirical relationships among magnitude, rupture length, rupture width, rupture area, and surface displacement, B. Seismol. Soc. Am., 84(4), 974–1002, 1994.

Wetzler, N., and Kurzon, I.: The earthquake activity in Israel: Revisiting 30 years of local and regional seismic records along the Dead Sea transform, Seismol. Res. Lett., 87(1), 47–58, 2016.

Wetzler, N., Sagy, A. and Marco, S.: The association of micro-earthquake clusters with mapped faults in the Dead Sea basin, J. Geophys. Res.: Solid Earth, 119(11), 8312–8330, 2014.

Woo, G.: Kernel estimation methods for seismic hazard area source modelling, B. Seismol. Soc. Am., 86(2), 353–362, 1996.

Zilberman, E., Baer. G., Avni, Y., and Feigin, D.: Pliocene fluvial systems and tectonics in the central Negev, southern Israel, Israel Journal of Earth Sciences, 45, 113–126, 1996.

Zilberman, E., Greenbaum, N., Nahmias, Y., and Porat, N.: The evolution of the northern shutter ridge, Mt. Carmel, and its implications on the tectonic activity along the

Yagur fault, Geological Survey of Israel Report No. GSI/14/2011, Jerusalem, 25 pp., 2011.

Zoback, M. L.: First-and second-order patterns of stress in the lithosphere: The World Stress Map Project, J. Geophys. Res.: Solid Earth, 97(B8), 11703–11728, 1992.

Zohar, M., Salamon, A. and Rubin, R.: Reappraised list of historical earthquakes that affected Israel and its close surroundings: J. Seismol., 20(3), 971–985, 2016.

Table 1: Main strike-slip faults: average slip rate details

Fault	~~Strike-~~ Lateral slip rate [mm/yr]	Data	Period	Reference
~~Aragonese [ARF]~~	~~5*~~	~~GPS~~	~~Recent~~	~~Baer et al. 1999; Hamiel et al., 2018a~~
Arava [AF]	4.9#±0.5# 4.5±0.9!	GPS Geology	Recent 37±5ka	Masson et al., 2015 Le Béon et al., 2010
Evrona [EF]	5.0±0.8#	GPS	Recent	Hamiel et al., 2018a
Gulf of Elat zone	4.5±0.3* (E 2.2±0.4)	GPS	Recent	Reilinger et al., 2006
Jericho ~~-~~[JF]	4.8±0.7#!# (E ~0.8)	GPS	Recent	Hamiel et al., 2018b
Jordan Valley [JVF] (south)	4.9±0.2#	Geology	~48ka	Ferry et al., 2007
Jordan Valley [JVF] (~~central~~centre)	~~5~~4.9±0.3#	Geology	~25ka	Ferry et al., 2011
Jordan Valley ~~(South to Sea of Galilee~~[JVF] (north)	4.1±0.~~8~~6#&	GPS	Recent	Hamiel et al., 2016
Jordan Gorge [JGF]	4.1±0.8# ~3# ~2.6#	GPS Geology Archaeology	Recent ~5ka ~3ka	Hamiel et al., 2016 Marco et al., 2005 Ellenblum et al., 2015
Lebanon Restraining Bend (LRB) zone	3.8±0.3* (C 1.6±0.4)	GPS	Recent	Gomez et al., 2007
Qiryat Shemona	3.9±0.3~~*~~!* (E 0.9±0.4)	GPS	Recent	Gomez et al., 2007
Roum [RF]	0.86–1.05#	Geology	Holocene	Nemer and Meghraoui, 2006
Serghaya [SF]	1.4±0.2#	Geology	Holocene	Gomez et al., 2003
~~Yammuneh (LRB – northern part)~~	~~2.8±0.5~~	~~GPS~~	~~Recent~~	~~Gomez et al., 2003; 2007~~
Yammuneh [YF] (north of LRB)	6.9±0.1# 4.2±0.3*	Geology GPS	2ka Recent	Meghraoui et al., 2003 Gomez et al., 2007

Geodetic or geological measurements on a specific segment~~.~~

~~! 0.8 mm/yr of extension normal to the fault~~

! The upper part of the interval is preferred by the authors (field considerations)

* According to geodetic-based model

& ~~Partially~~E, C extension and convergence, respectively, normal to the fault

& creeping from a depth of 1.5 ± 1.0 km to the surface at a rate of 2.5 ± 0.8 mm/yr

Table 2. Marginal faults and branches with integrated slip or subsidence of ~ 0.5~~ mm/yr~~ ~~≤ VS ≤ ~~ ~ 1 mm/yr and references

Fault	Slip rate [mm/yr]	Data	Period	Reference
Dead Sea basin marginal faults	≥1 Based on basin subsidence rates	Geology Geophysics	Pleistocene-Holocene	Bartov and Sagy, 2004; Torfstein et al., 2009; ten Brink and Flores, 2012~~;~~ ~~Bartov and Sagy, 2004~~
~~Carmel-Tirza-Izrael fault zone [CTF]~~ Carmel	0.9±0.45 ~~total~~Total slip rate (0.7±0.45 lateral; 0.6±0.45 extension) < 0.5	GPS Geology	Recent 200ka	Sadeh et al., 2012 Zilberman et al., 2011
Hula western border	~~>~~ ~0.4 Based on basin subsidence rates	Geology Geophysics	~1 Ma	Schattner and Weinberger, 2008
Elat	?	Geology	Holocene	~~Amit et al., 2002;~~ Porat et al., 1996; Amit et al., 2002; Shaked et al., 2004

Figure captions

Figure 1: ~~-~~Plate configuration in the Eastern Mediterranean. Arrows show relative motion. SR- Suez Rift; GEA~~:~~- Gulf of Elat/Aqaba~~.~~; DST- Dead Sea Transform fault system; CTF- Carmel Tirza Fault zone; LRB- Lebanon Restraining Bend; CA- Cyprian Arc; DSB- Dead Sea basin; SG- Sea of Galilee.

Figure 2: Epicentres in Israel and surrounding areas between the years 1983-2017, based on the relocated earthquake catalogue. Circle size and colours indicate the magnitude. Black lines represent the main fault segments of the DST and the CTF. ~~The background for this figure and the followings is based on Farr et al., (2007).~~

Figure 3: The *earthquake kernel density* distribution, according to the relocated catalogue. Colours and corresponding numbers indicate the value in [events/km^2/yr].

Figure 4: The *seismic moment kernel density* distribution, according to the relocated catalogue. Colours and corresponding numbers indicate the value in $log[joule/km^2/yr]$.

Figure 5: The main seismic sources in Israel and adjacent areas. Colours indicate the two categories of faults according to the criteria. Inferred subsurface faults are marked by dashed lines. Abbreviations are for the DST main strike-slip segments, its main branches and marginal faults. Numbers indicate geodetic slip rates [mm/yr] for strike-slip components~~,~~ according to recent studies (for errors and longer-term slip rates, see Tables 1, 2~~).~~; Fig. A3). Brackets indicate slip rates accommodated by an entire fault zone. Asterisk denotes segments of unknown slip rates, where the fault splits into a few (sub-) parallel segments.

Figure 6. The seismicity polygons: earthquake density of values > ~0.001[events/km^2/yr] and Mo density of values > ~9.5 $log[joule/km^2/yr]$; the product is the overlap polygon (in brown).

Figure 7. Quaternary fault map of Israel. Colours indicate the corresponding criterion for each fault. Inferred subsurface faults are marked by dashed lines. Abbreviations are for the main strike-slip segments of the DST.

32⁰0'0''E
36⁰0'0''E
Anatolian plate
DST N. Regime
CA
34⁰0'0''E
LRB
Deep Levant
Basin
CTF
Mediterranean
Sea
Sinai subplate
DST S. Regime
30⁰0'0''E
Arabian
plate
GEA
SR
African
plate
Red Sea
0 37.5 75 150
Km

~~Figure 1~~

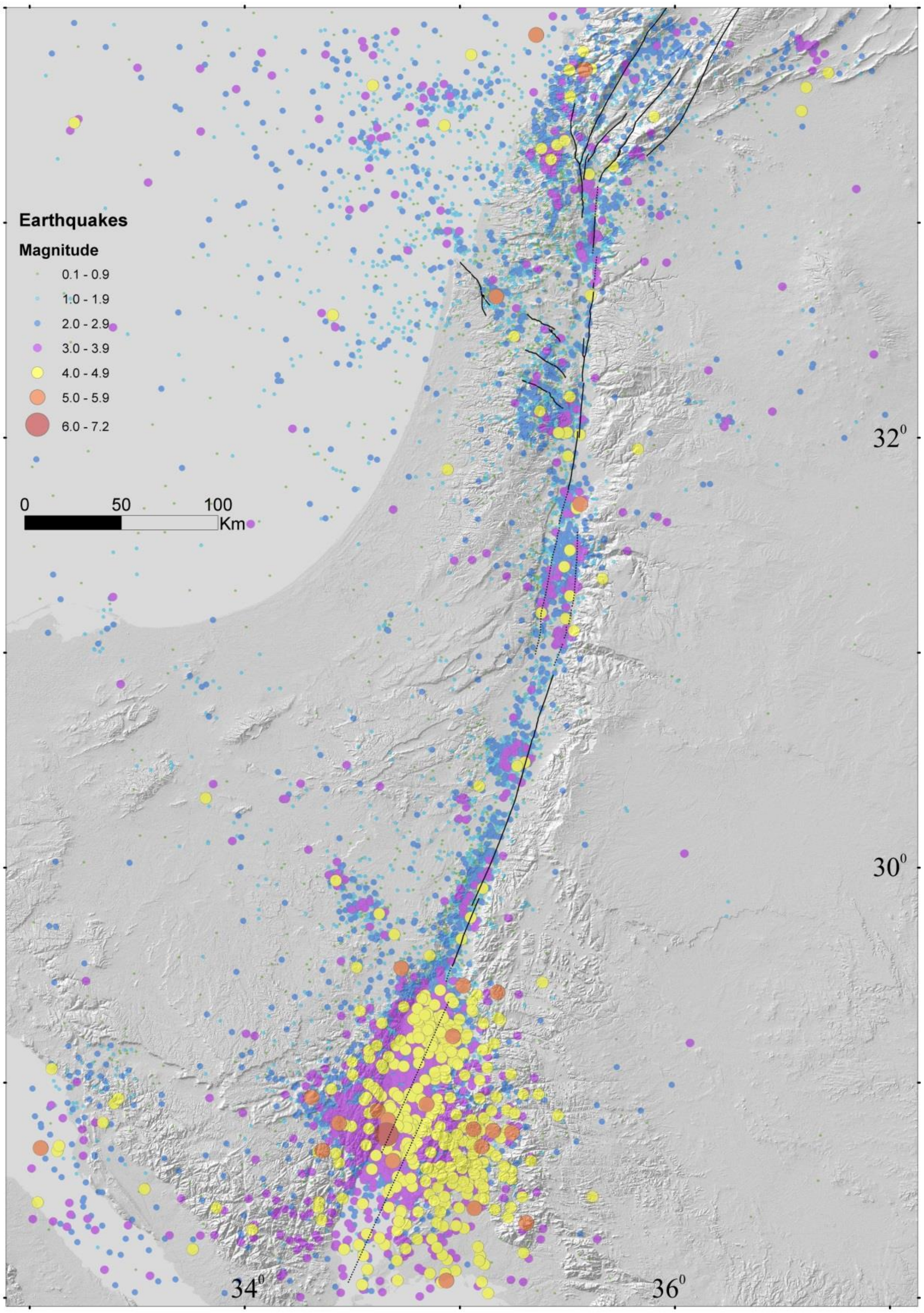
Earthquakes
Magnitude
0.1 - 0.9
1.0 - 1.9
2.0 - 2.9
3.0 - 3.9
4.0 - 4.9
5.0 - 5.9
6.0 - 7.2
0
50
100
Km
32°
30°
34°
36°

~~Figure 2~~

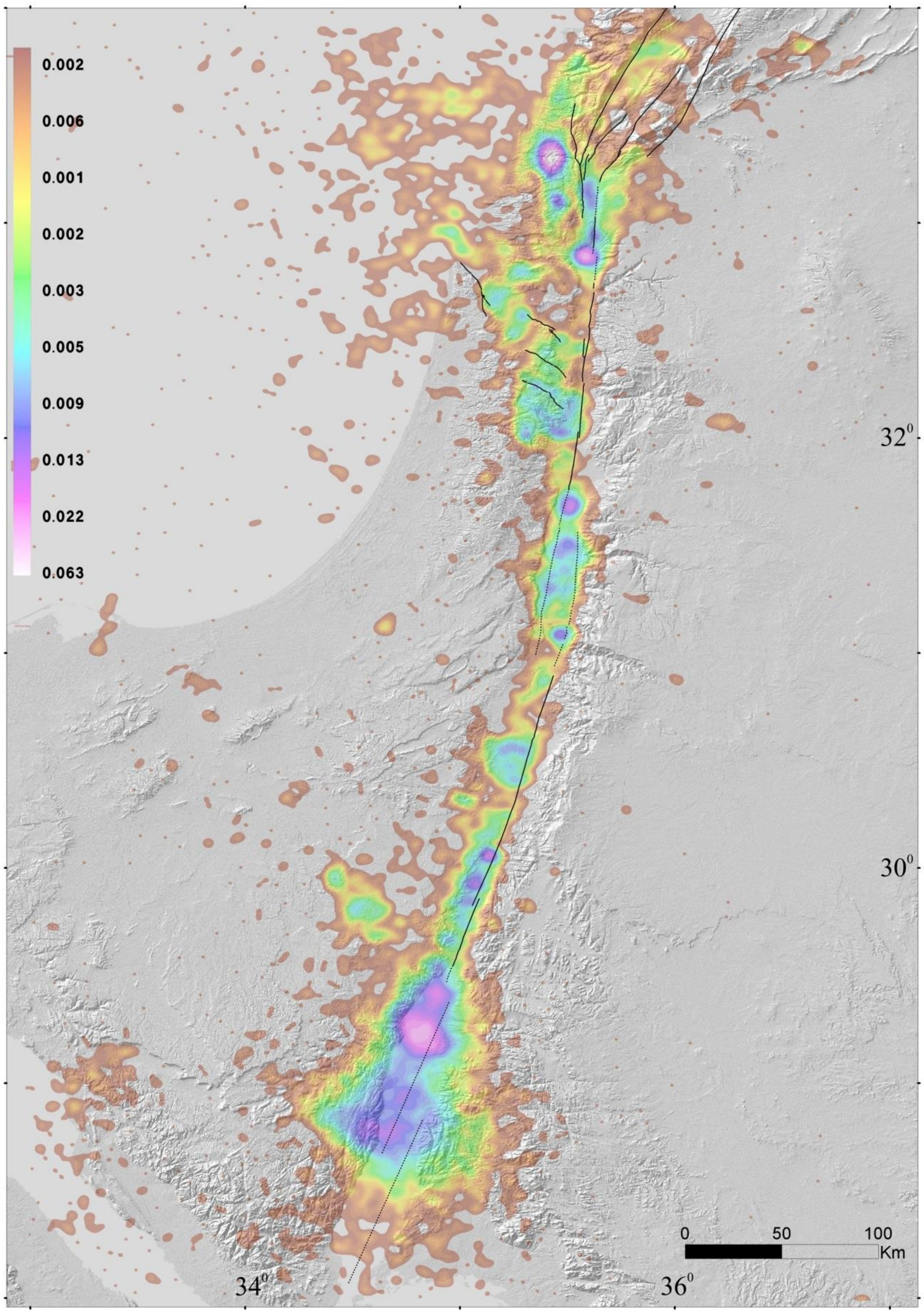

0.002
0.006
0.001
0.002
0.003
0.005
0.009
0.013
0.022
0.063
32⁰
30⁰
34⁰
36⁰
0
50
100
Km

~~Figure 3~~

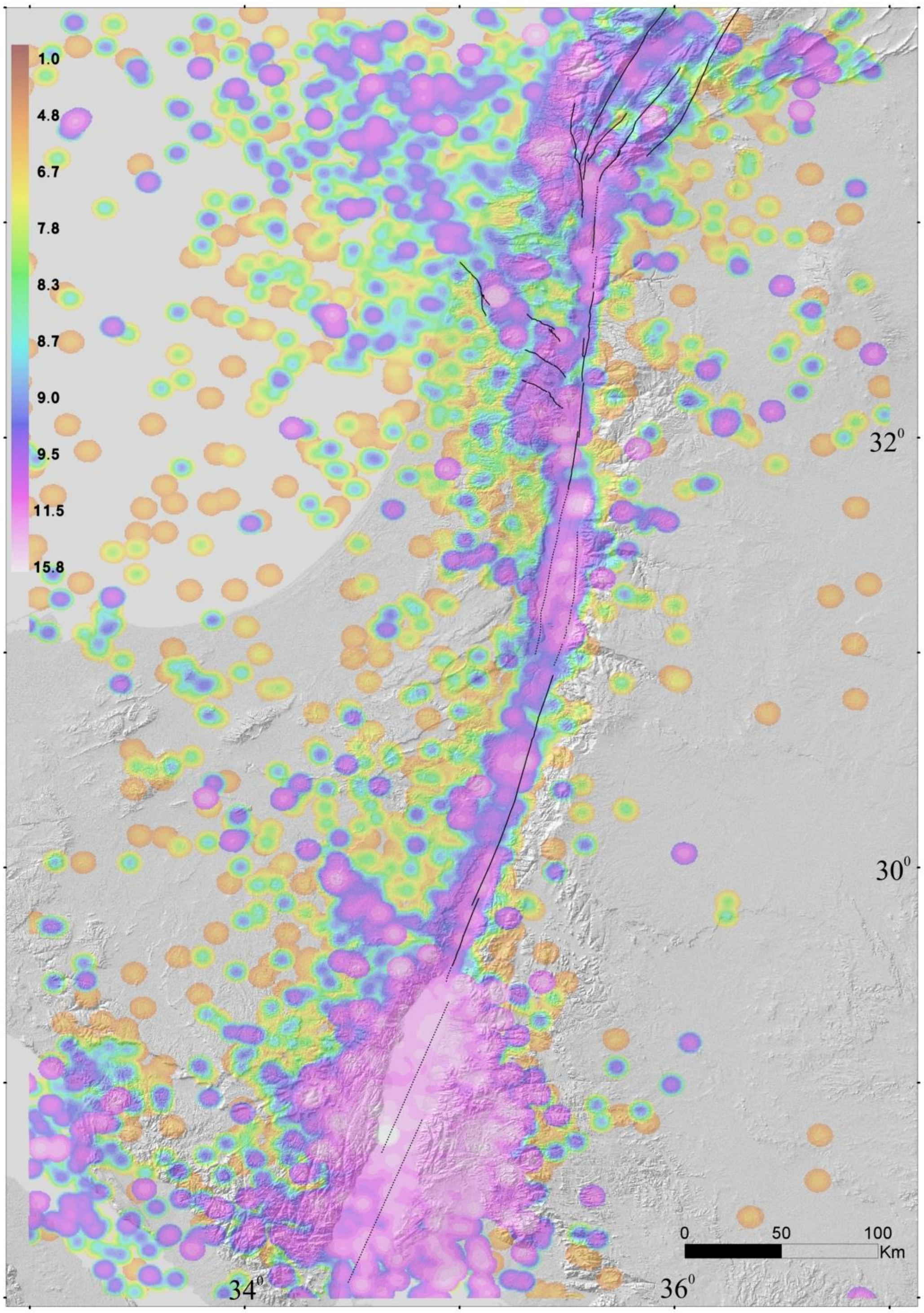

~~Figure 4~~

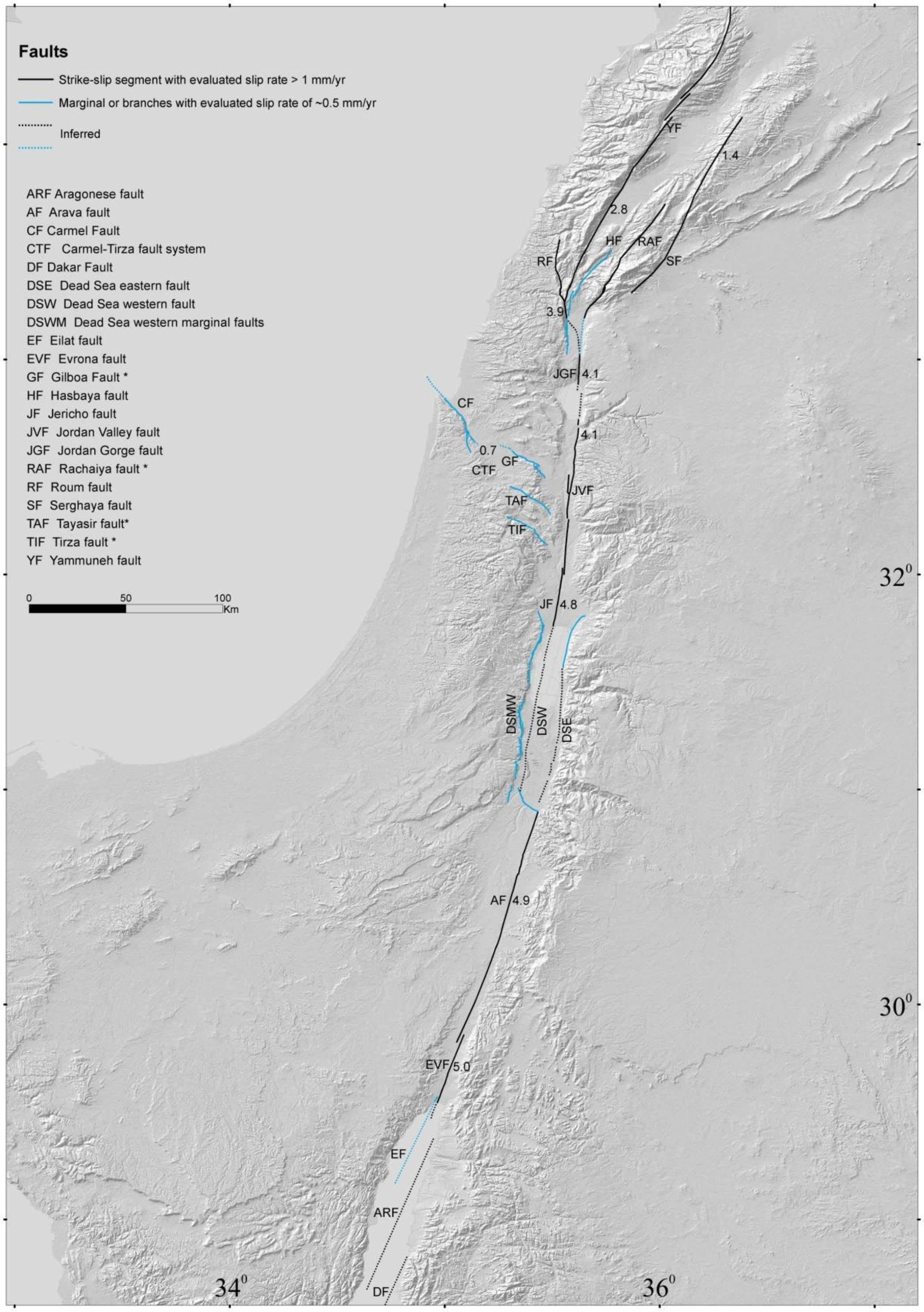
Faults
Strike-slip segment with evaluated slip rate > 1 mm/yr
Marginal or branches with evaluated slip rate of ~0.5 mm/yr
Inferred
ARF Aragonese fault
AF Arava fault
CF Carmel Fault
CTF Carmel-Tirza fault system
DF Dakar Fault
DSE Dead Sea eastern fault
DSW Dead Sea western fault
DSWM Dead Sea western marginal faults
EF Eilat fault
EVF Evrona fault
GF Gilboa Fault *
HF Hasbaya fault
JF Jericho fault
JVF Jordan Valley fault
JGF Jordan Gorge fault
RAF Rachaiya fault *
RF Roum fault
SF Serghaya fault
TAF Tayasir fault*
TIF Tirza fault *
YF Yammuneh fault
0
50
100
Km
YF
1.4
2.8
HF
RAF
SF
RF
3.9
JGF 4.1
CF
4.1
0.7
GF
CTF
JVF
TAF
TIF
32⁰
JF 4.8
DSMW
DSW
DSE
AF 4.9
30⁰
EVF 5.0
EF
ARF
34⁰
36⁰
DF

~~Figure 5~~

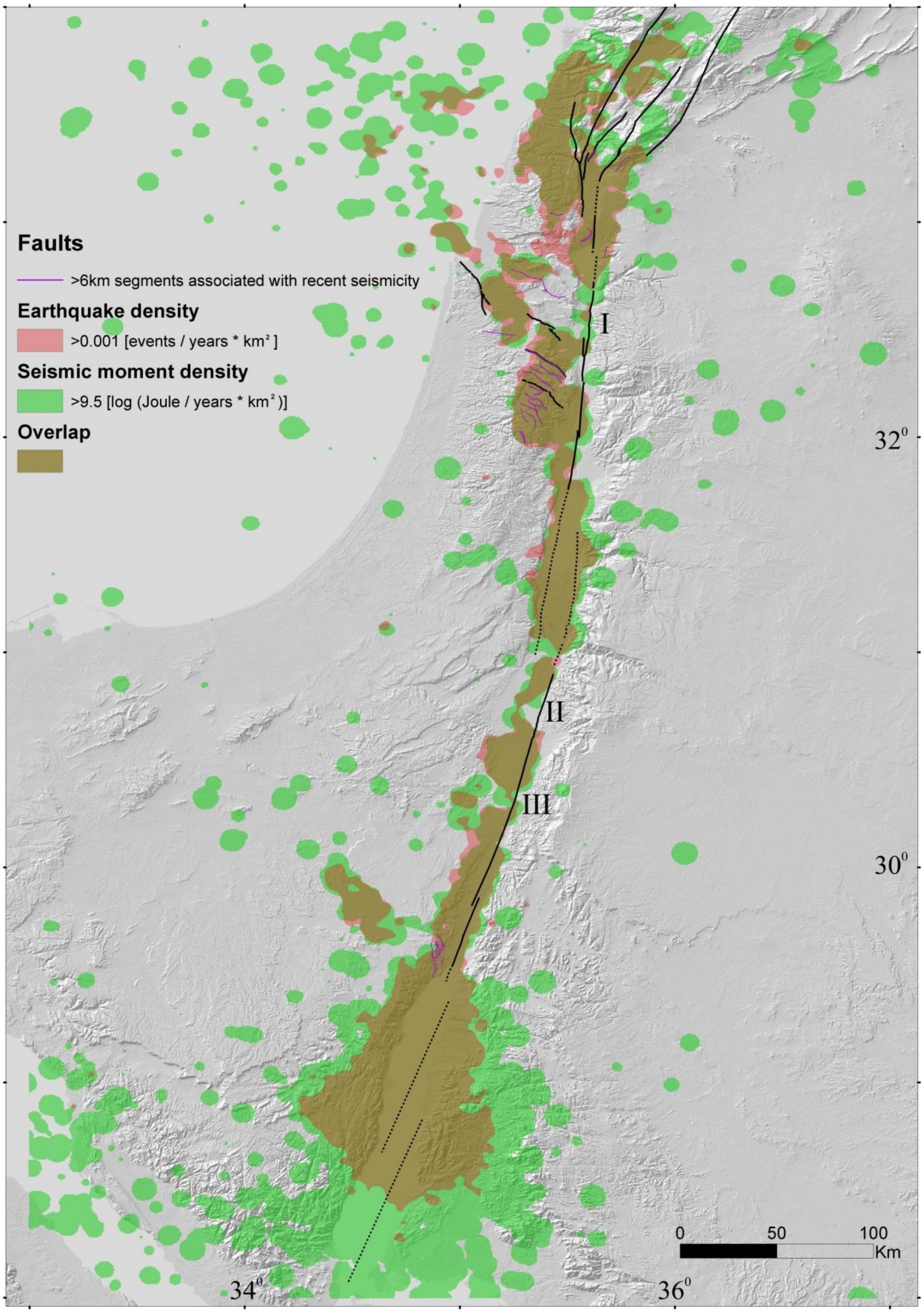
Faults
>6km segments associated with recent seismicity
Earthquake density
>0.001 [events / years * km²]
Seismic moment density
>9.5 [log (Joule / years * km²)]
Overlap
I
II
III
32⁰
30⁰
34⁰
36⁰
0
50
100
Km

~~Figure 6~~

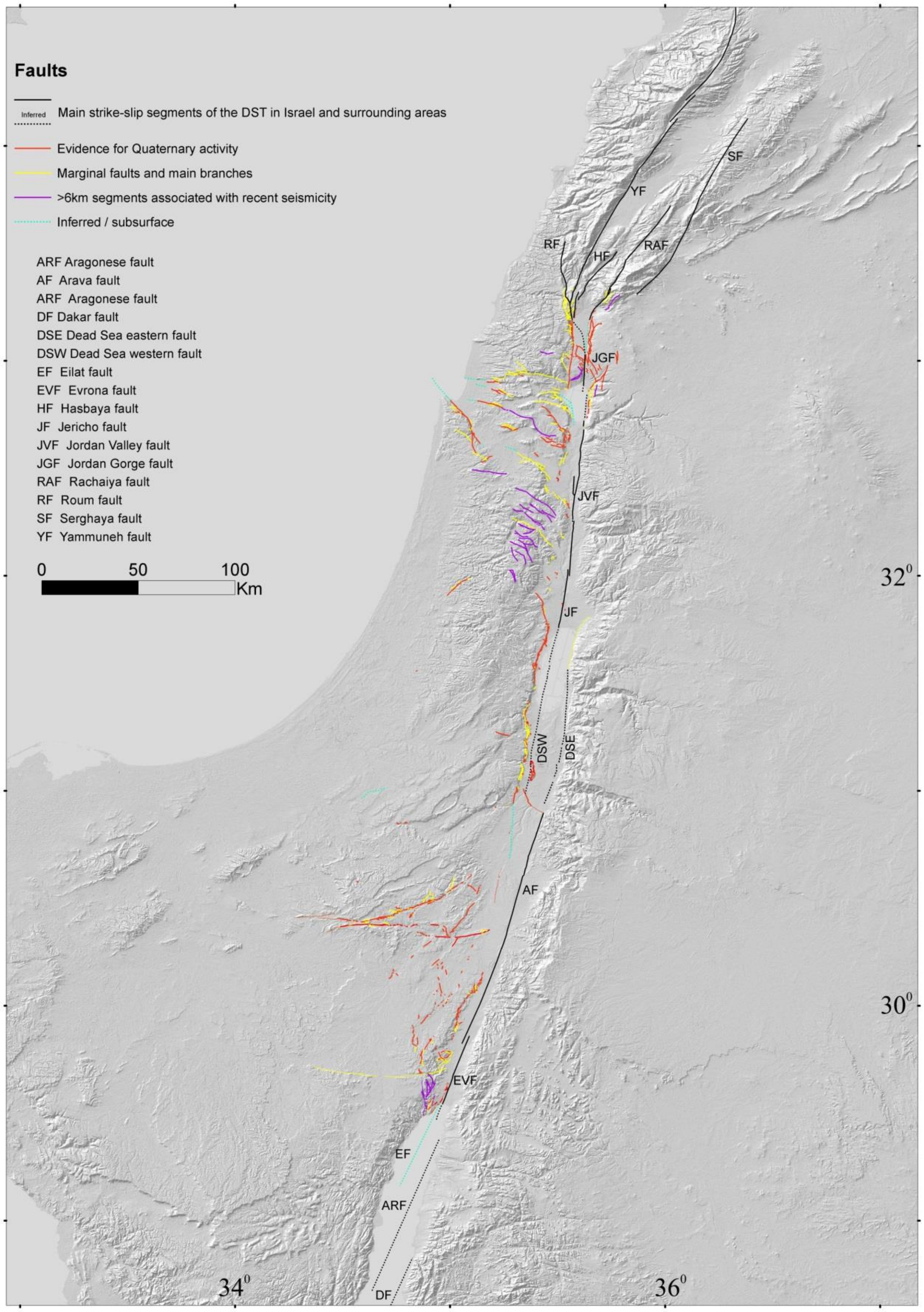
Faults
Inferred
Main strike-slip segments of the DST in Israel and surrounding areas
Evidence for Quaternary activity
Marginal faults and main branches
>6km segments associated with recent seismicity
Inferred / subsurface
ARF Aragonese fault
AF Arava fault
ARF Aragonese fault
DF Dakar fault
DSE Dead Sea eastern fault
DSW Dead Sea western fault
EF Eilat fault
EVF Evrona fault
HF Hasbaya fault
JF Jericho fault
JVF Jordan Valley fault
JGF Jordan Gorge fault
RAF Rachaiya fault
RF Roum fault
SF Serghaya fault
YF Yammuneh fault
0
50
100
Km
SF
YF
RF
HF
RAF
JGF
JVF
32°
JF
DSW
DSE
AF
30°
EVF
EF
ARF
DF
34°
36°

~~Figure 7~~

~~Appendix 1~~

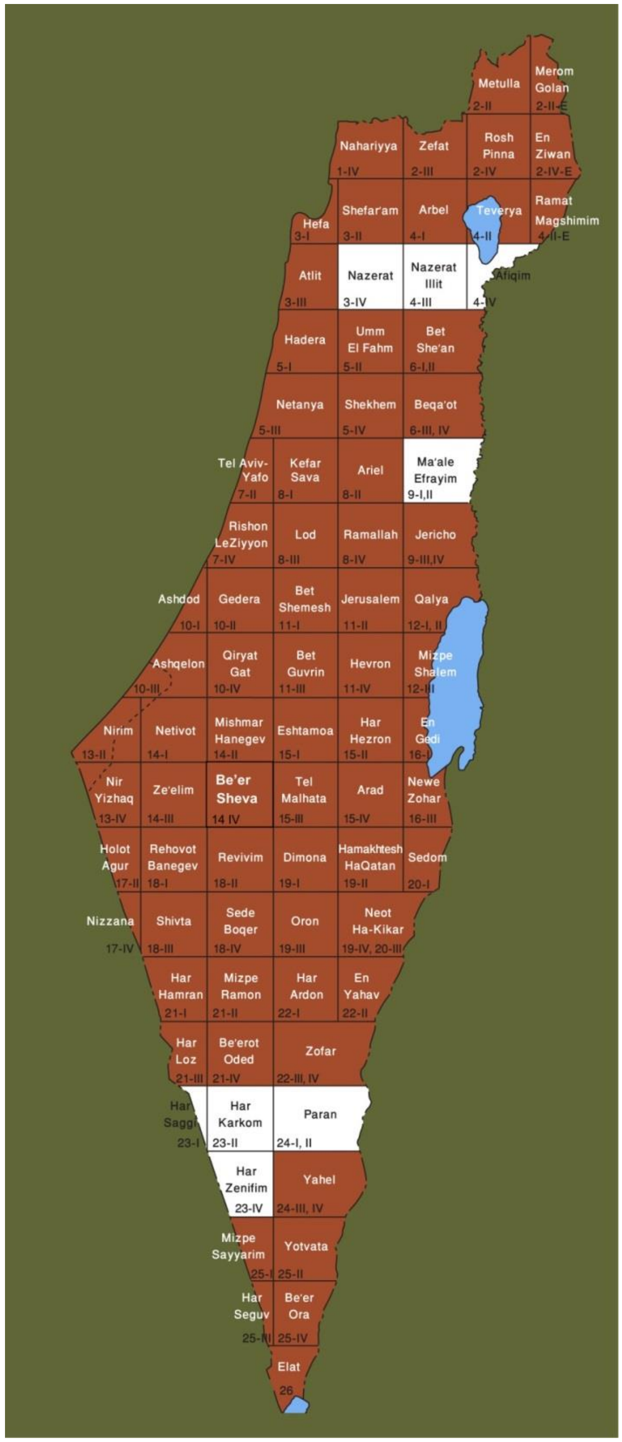

Figure A1. Locations of the 1:50,000 geological map sheets used for the present map (as of August 2018). Brown: locations of published 1:50,000 sheets. White: unpublished sheets.

Figure A2. Seismic stations utilised for recording the earthquakes of the examined catalogue, and the ensuing seismic network coverage area. The spatial distribution of the

stations is temporal dependent. Stations that recorded less than 350 arrivals are in black, while stations that recorded more than 350 arrivals are in blue. Green lines mark the borders of the seismic network coverage area as defined in this study.

Figure A3: The main seismic sources in Israel and adjacent areas as in Fig. 5, with colours indicating the two fault categories according to the criteria. Inferred subsurface faults are marked by dashed lines. Abbreviations are for the DST main strike-slip segments, its main branches and marginal faults. Numbers indicate lateral components of slip rates [mm/yr] according to geodetic investigations (black) and field measurements of lateral offsets (green), based on recent studies (Tables 1, 2). Brackets indicate slip rates accommodated by an entire fault zone. Asterisk denotes segments of unknown slip rates, where the fault splits into a few (sub-) parallel segments.

Figure A4. Quaternary faults superimposed on the seismicity polygons of the seismicity-based criterion. The letter S indicates on SNB faults.

Figure A5. Marked ~NW trending seismicity lineaments: CTF (north) and the EBL (south), on the distribution maps of the *earthquake density* (a) and *seismic moment density* (b), as in Figs. 3, 4.

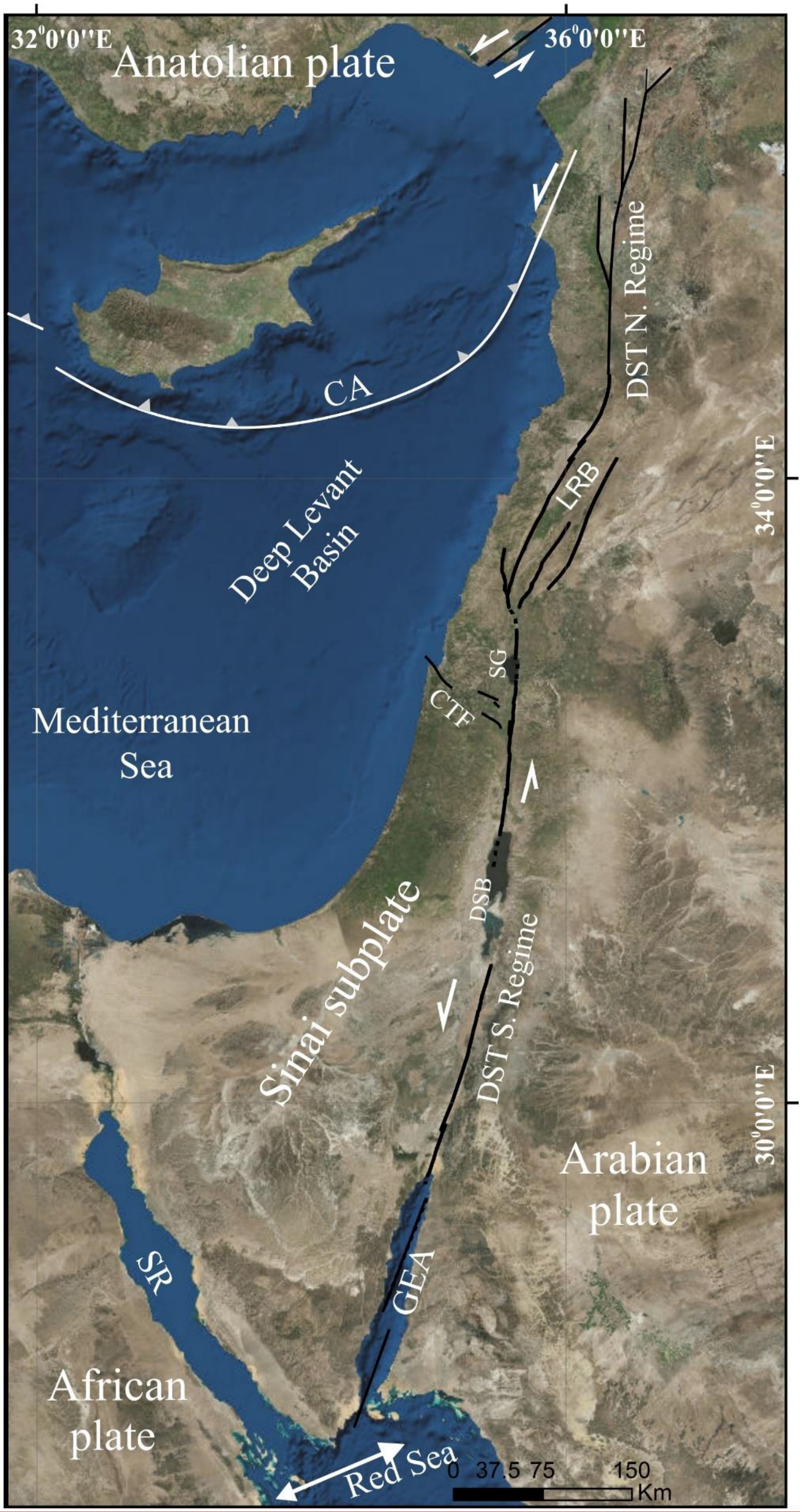

32°0'0''E
36°0'0''E
34°0'0''E
30°0'0''E
Anatolian plate
CA
DST N. Regime
LRB
Deep Levant Basin
SG
CTF
Mediterranean Sea
DSB
Sinai subplate
DST S. Regime
Arabian plate
SR
GEA
African plate
Red Sea
0 37.5 75 150
Km

Figure 1

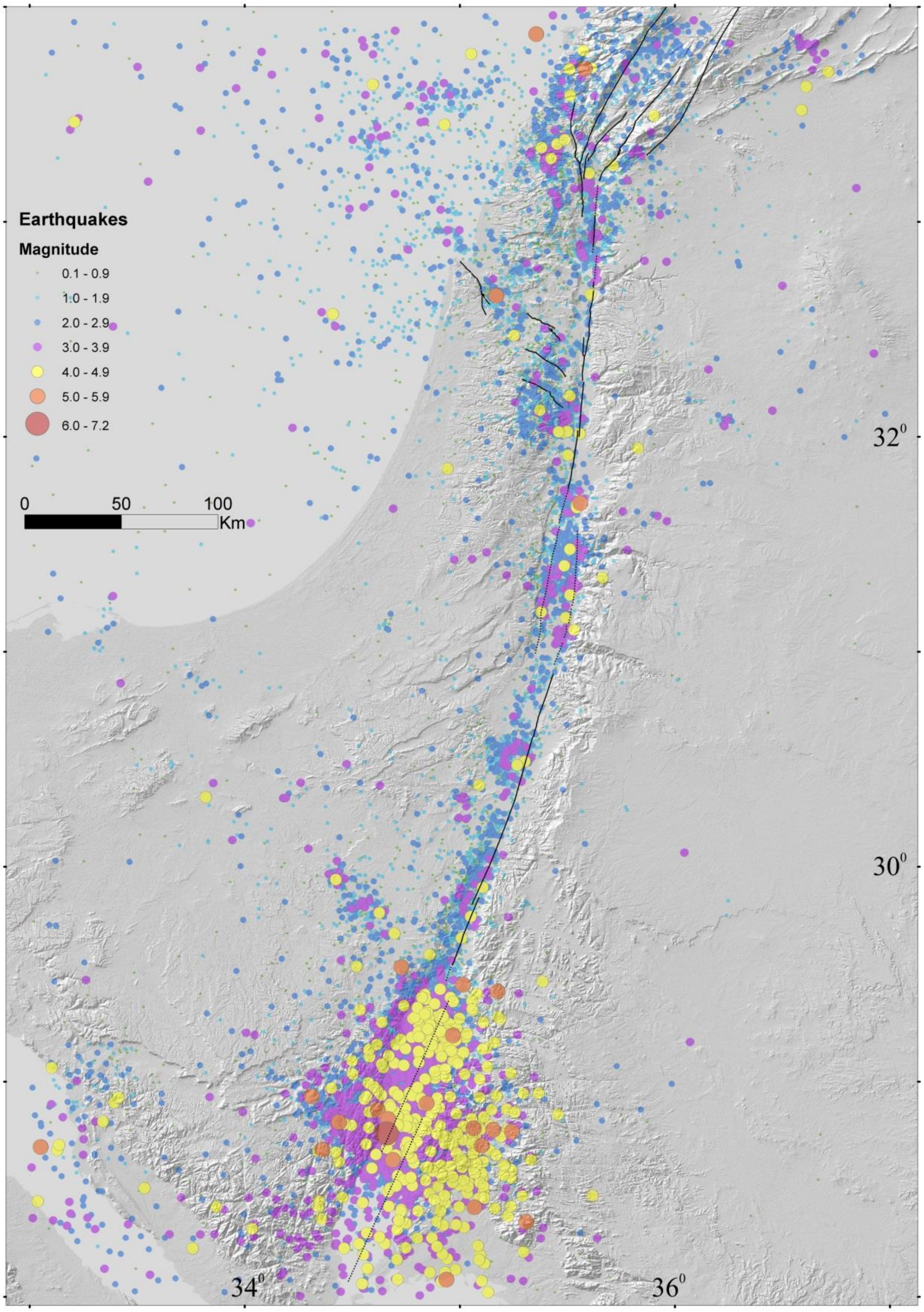

Figure 2

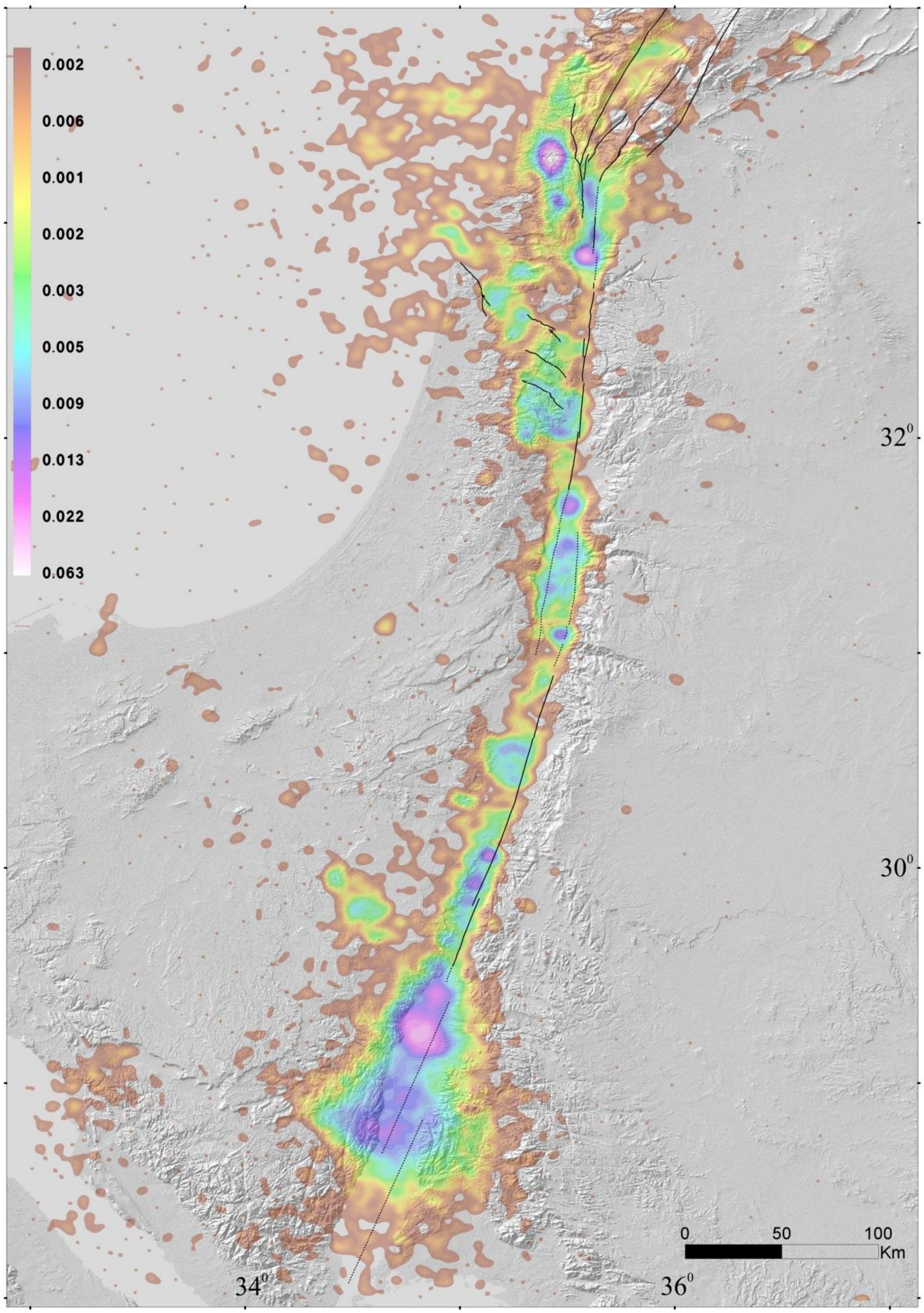
0.002
0.006
0.001
0.002
0.003
0.005
0.009
0.013
0.022
0.063
32⁰
30⁰
34⁰
36⁰
0
50
100
Km

Figure 3

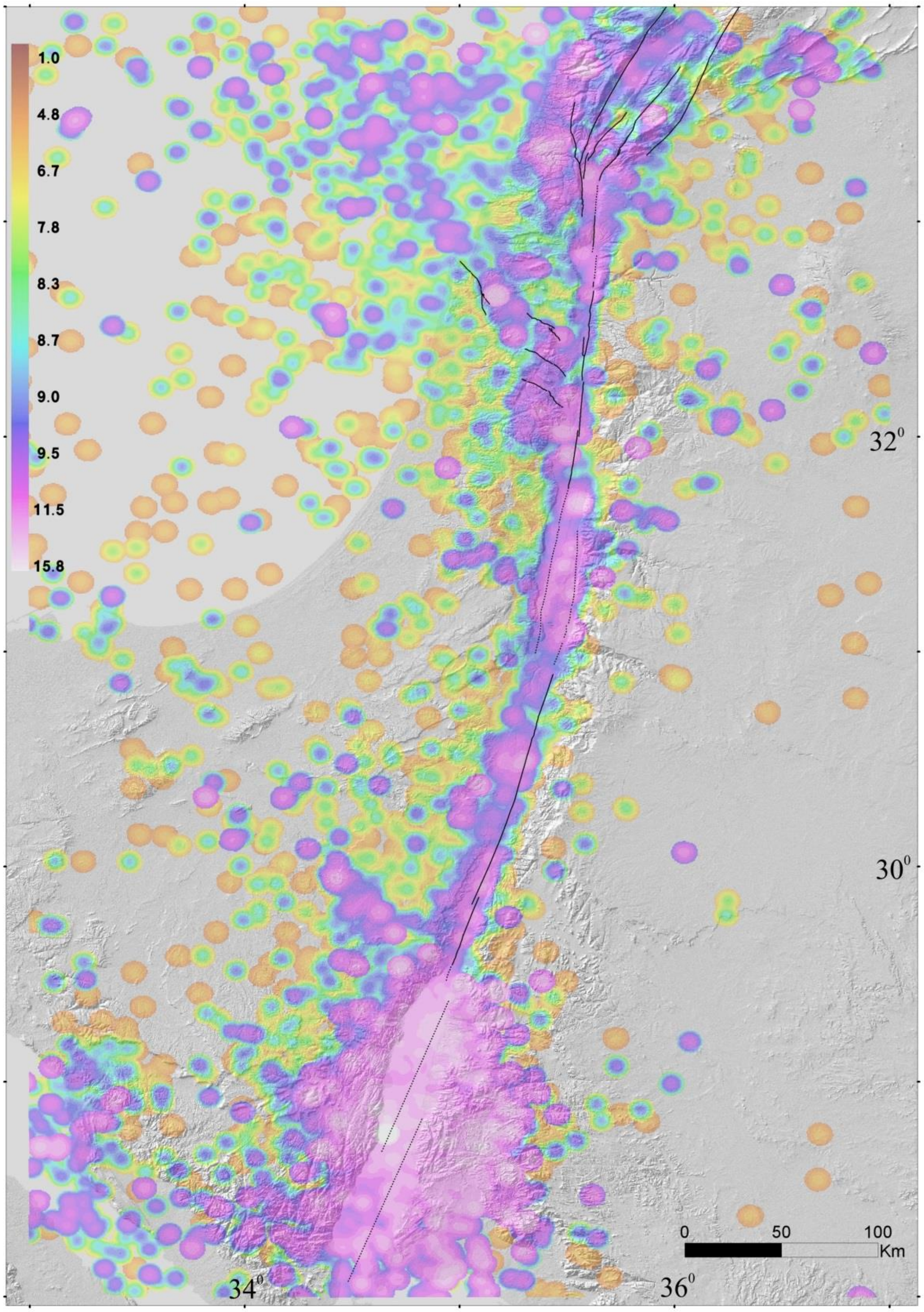

Figure 4

1382

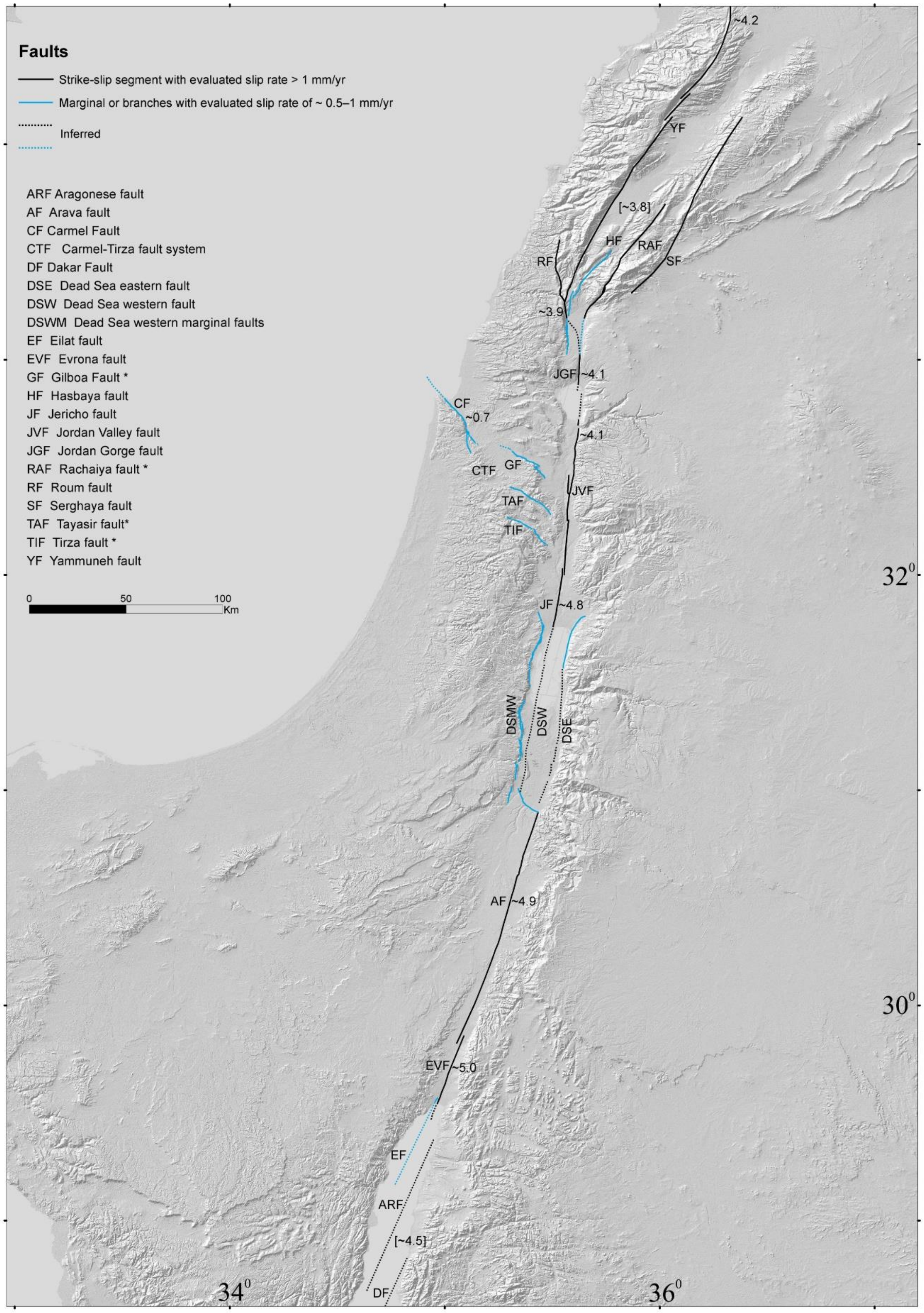

1383 **Figure 5**

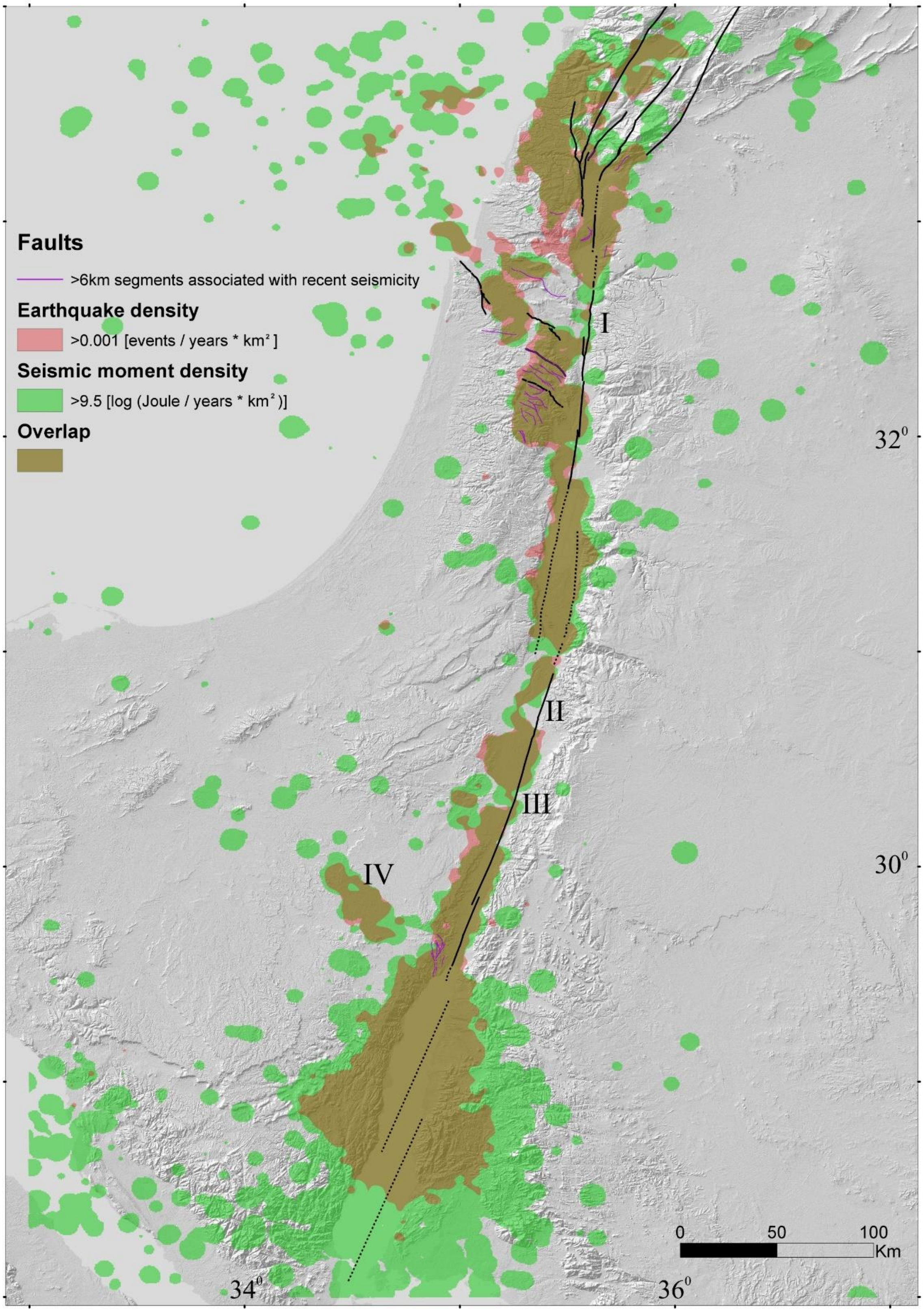
Faults
>6km segments associated with recent seismicity
Earthquake density
>0.001 [events / years * km²]
Seismic moment density
>9.5 [log (Joule / years * km²)]
Overlap
I
II
III
IV
32⁰
30⁰
34⁰
36⁰
0 50 100
Km

Figure 6

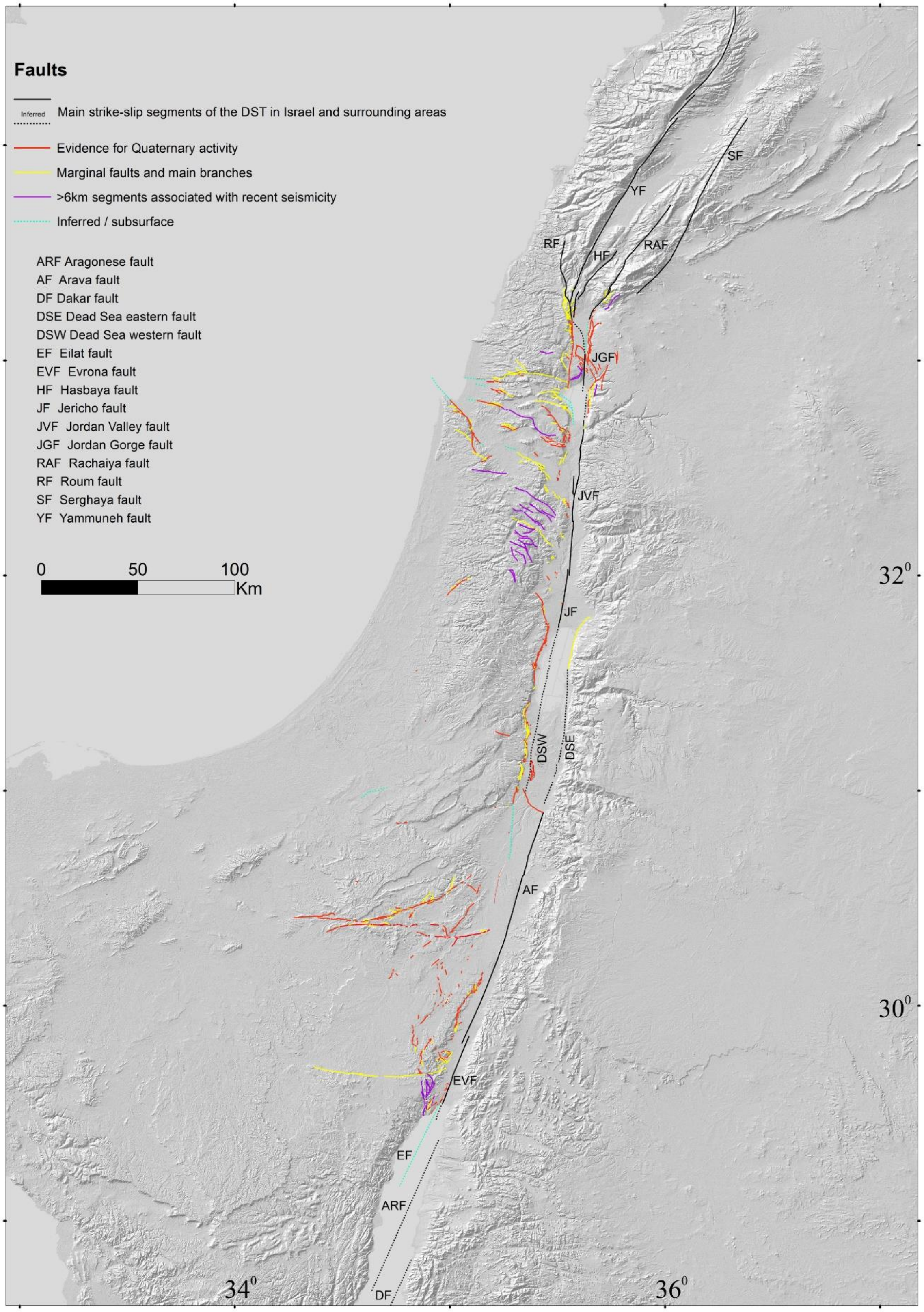
Faults
Inferred
Main strike-slip segments of the DST in Israel and surrounding areas
Evidence for Quaternary activity
Marginal faults and main branches
>6km segments associated with recent seismicity
Inferred / subsurface
ARF Aragonese fault
AF Arava fault
DF Dakar fault
DSE Dead Sea eastern fault
DSW Dead Sea western fault
EF Eilat fault
EVF Evrona fault
HF Hasbaya fault
JF Jericho fault
JVF Jordan Valley fault
JGF Jordan Gorge fault
RAF Rachaiya fault
RF Roum fault
SF Serghaya fault
YF Yammuneh fault
0
50
100
Km
SF
YF
RF
HF
RAF
JGF
JVF
JF
DSW
DSE
AF
EVF
EF
ARF
DF
32^0
30^0
34^0
36^0

Figure 7

Appendix 1

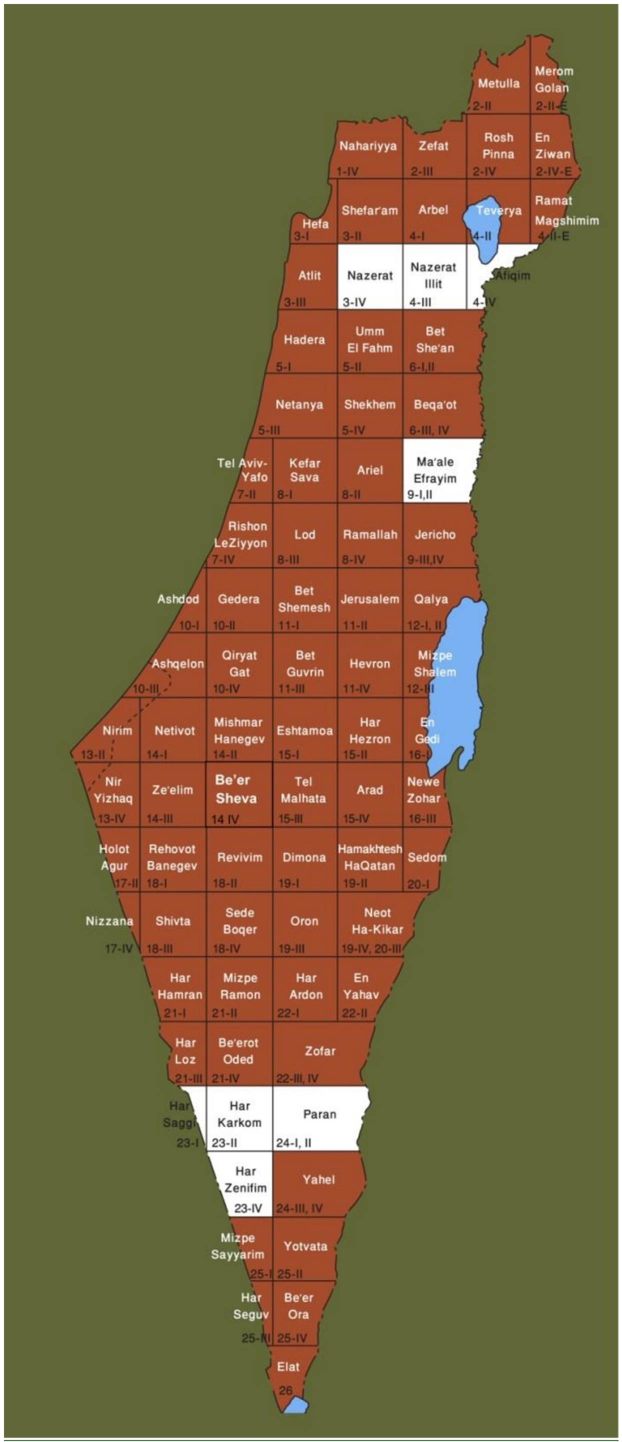

Figure A1

Table A1: References for faults and fault segments that have been marked based on papers, reports, and theses. Faults are listed in table 3 if their latest mapping is not updated yet in the 1:50,000 sheets (as of 2018), or if their definition as Quaternary faults cannot be directly deduced from the geological maps. Fault names are mainly according to the references.

Area	Name of fault / group of faults or segments	References
Southern Israel	Arif-Bator	Zilberman et al., 1996; Avni, 1998
	Gerofit	Ginat, 1997
	Gevaot Ziya	Avni, 1998
	Halamish line	Avni, 1998
	Har Seguv	Avni, 1998
	Hiyyon	Ginat, 1997
	Katzra	Avni, 1998
	Milhan	Ginat, 1997
	Mitzpe Sayarim	Avni, 1998
	Noza	Ginat, 1997
	Ovda	Avni, 1998
	Paran	Zilberman, 1985; Avni, 1998; Calvo et al., 1998; Calvo, 2002
	Yotam	Wieler et al., 2017
	Zhiha	Avni, 1998
	Zin	Enzel et al., 1988; IEC and WLA, 2002; Avni and Zilberman, 2007
	Znifim – Zihor – Barak	Ginat, 1997
	Zofar	Calvo, 2002
Central Israel and Dead Sea area	Jericho	Sagy and Nahmias, 2011
	Masada Plain	Bartov et al., 2006
	Modi'in	Buchbinder and Sneh, 1984
	Nahal Darga (east)	Enzel et al., 2000
	Nahal Kidron (east)	Sagy and Nahmias, 2011
Northern Israel	Ahihud	Kafri and Ecker, 1964; Zilberman et al., 2011
	Beit Qeshet (western part)	Zilberman et al., 2009
	Ha'on	Katz et al., 2009
	Hilazon	Kafri and Ecker, 1964; Zilberman et al., 2008
	Kabul	Kafri and Ecker, 1964; Zilberman et al., 2008
	Nahef East Fault	Mitchell et al., 2001
	Nesher	Zilberman et al., 2006; 2008
	Tiberias	Marco et al., 2003

Table A2: List of geological formations and units used for the ~~QFMI~~Quaternary fault map of Israel. Geologic and geomorphic descriptions that appear in 1:50,000 geological maps for Quaternary deposits.

Formations	**Local sedimentary units**	**Local volcanic units**	**Other units***
Ahuzam Fm. (Cgl.)	Amora Salt	Avital Tuff	Alluvium
Arava Fm.	Betlehem Cgl.	Bene Yehuda Scoria	Beach rocks & reefs
Amora Fm.	Biq`at Uvda Cgl.	Brekhat Ram Tuff	Calcareous sandstone (kurkar)
Ashmura Fm.	Edom facias	Dalton Basalt	Colluvium
Garof Fm.	Egel Cgl.	Dalton Scoria & Tuff	Dune sand, Sand sheets, Red sands
Gesher Bnot Ya'aqov Fm.	En Awwazim Cgl.	Dalwe flows	Loess, fluvial & eolian
Hazor & Gadot Fms.	En Feshha Cgl.	En Awwazim flow	Gypsum
Lisan Fm.	Giv'at Oz Cgl.	En Zivan Basalt flows	Lake sediments
Malaha Fm.	Karbolet caprock	Golan Basalt flows (Muweissa and En Zivan flows)	Loam (hamra)
Mazar Fm.	Lot caprock	Hazbani Basalt flows	Neogene-Quaternary conglomerate units, Terrace cgl.
Nevatim Fm.	Mahanayim Marl	Keramim Basalt	Playa
Ortal Fm.	Mearat Sedom caprock	Meshki Basalt flows	Recent fan
Pleshet Fm.	Nahshon Cgl.	Muweisse Basalt flows	Soil
Samra Fm.	Ramat Gerofit Cgl.	Neogene Basalts	Tufa, travertine
Sede Zin Fm.	Ravid Cgl.	Raqad Basalt	Unnamed clastic unit
Seif Fm.	Ruhama Loess & sand	Sa'ar Basalt flows	
Ye'elim Fm.	Sabkha soil	Shievan Scoria	
Ze'elim Fm.	Si'on Cgl.	Yarda/Ruman Basalt flows	
Zehiha Fm.	Wadi Malih Cgl.	Yarmouk Basalt	
		Yehudiyya & Dalwe Basalt flows	

Table A3*: References for faults located beyond Israel borders and/or subsurface faults*

Geographic area	**Reference**
Gulf of Elat	Ben-Avraham, 1985; Hartman et al., 2014~~;~~
Arava valley	Calvo, 2002; Le Béon et al., 2012; Sneh and Weinberger, 2014
Sinai peninsula	Sneh and Weinberger, 2014
North-western Negev	Eyal et al., 1992
Dead Sea basin	Ben-Avraham and Schubert, 2006; Sneh and Weinberger, 2014
Jordan valley	Ferry et al., 2007; Sneh and Weinberger, 2014
Gilboa fault (western part)	Sneh and Weinberger, 2014
Carmel fault (eastern part)	Sneh and Weinberger, 2014
Carmel fault (western part)	Schattner and Ben-Avraham, 2007
Zvulun ~~Valley~~valley	Sagy and Gvirtzman, 2009
Sea of Galilee	Hurwitz et al., 2002; Reznikov et al., 2004; Eppelbaum et al., 2007; ~~-~~Sneh and Weinberger, 2014
Hula basin	Schattner and Weinberger, 2008
Lebanon and Syria	Weinberger et al., 2009; Garfunkel, 2014; Sneh and Weinberger, 2014

Table A3: References for faults located beyond Israel borders and/or subsurface faults

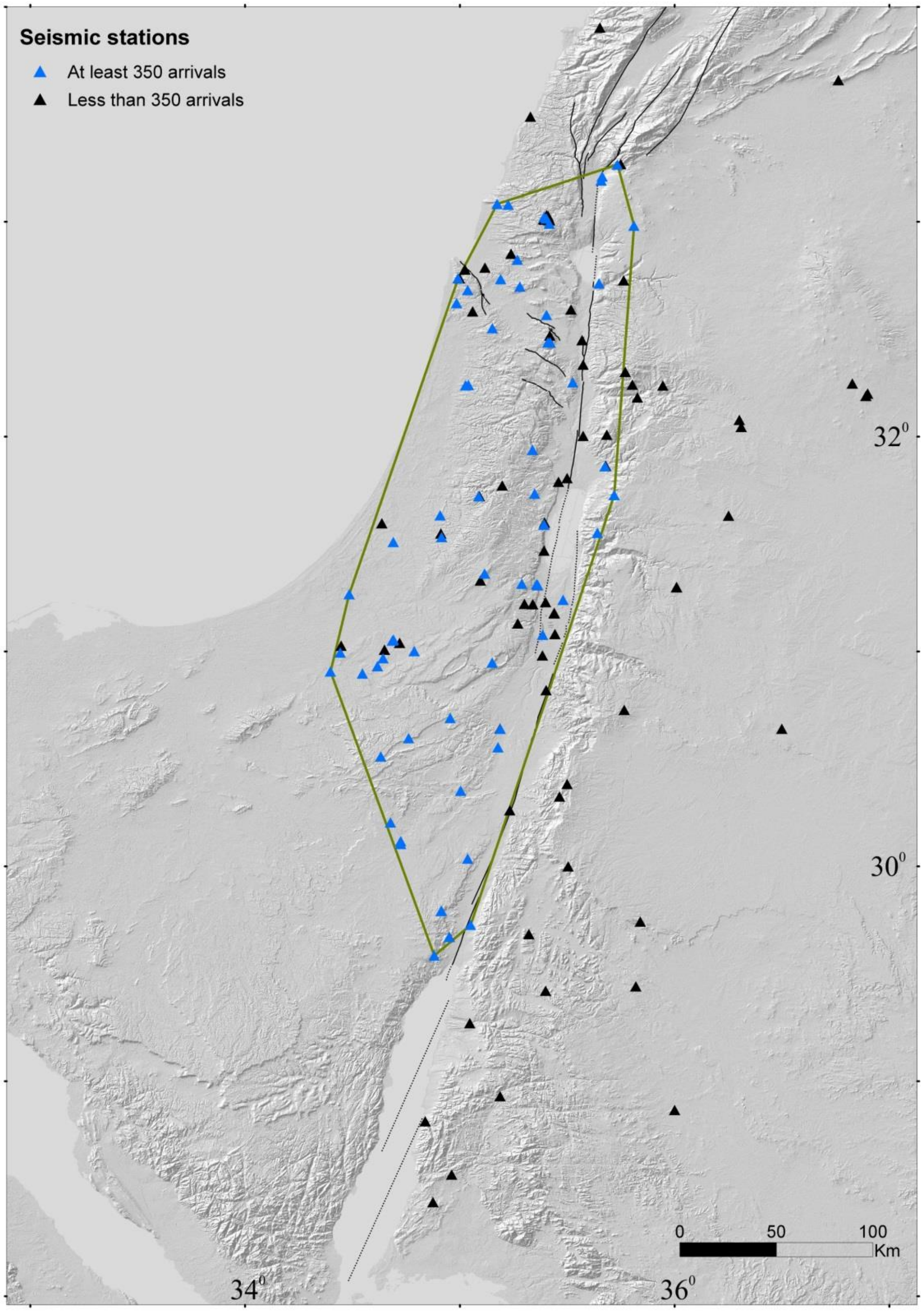

Figure A2~~. Seismic stations utilised for recording the earthquakes of the examined catalogue, and the ensuing seismic network coverage area. The spatial distribution of the stations is temporal dependent. Stations that recorded less than 350 arrivals are in black, while stations that recorded more than 350 arrivals are in blue. Green lines mark the borders of the seismic network coverage area as defined in this study.~~

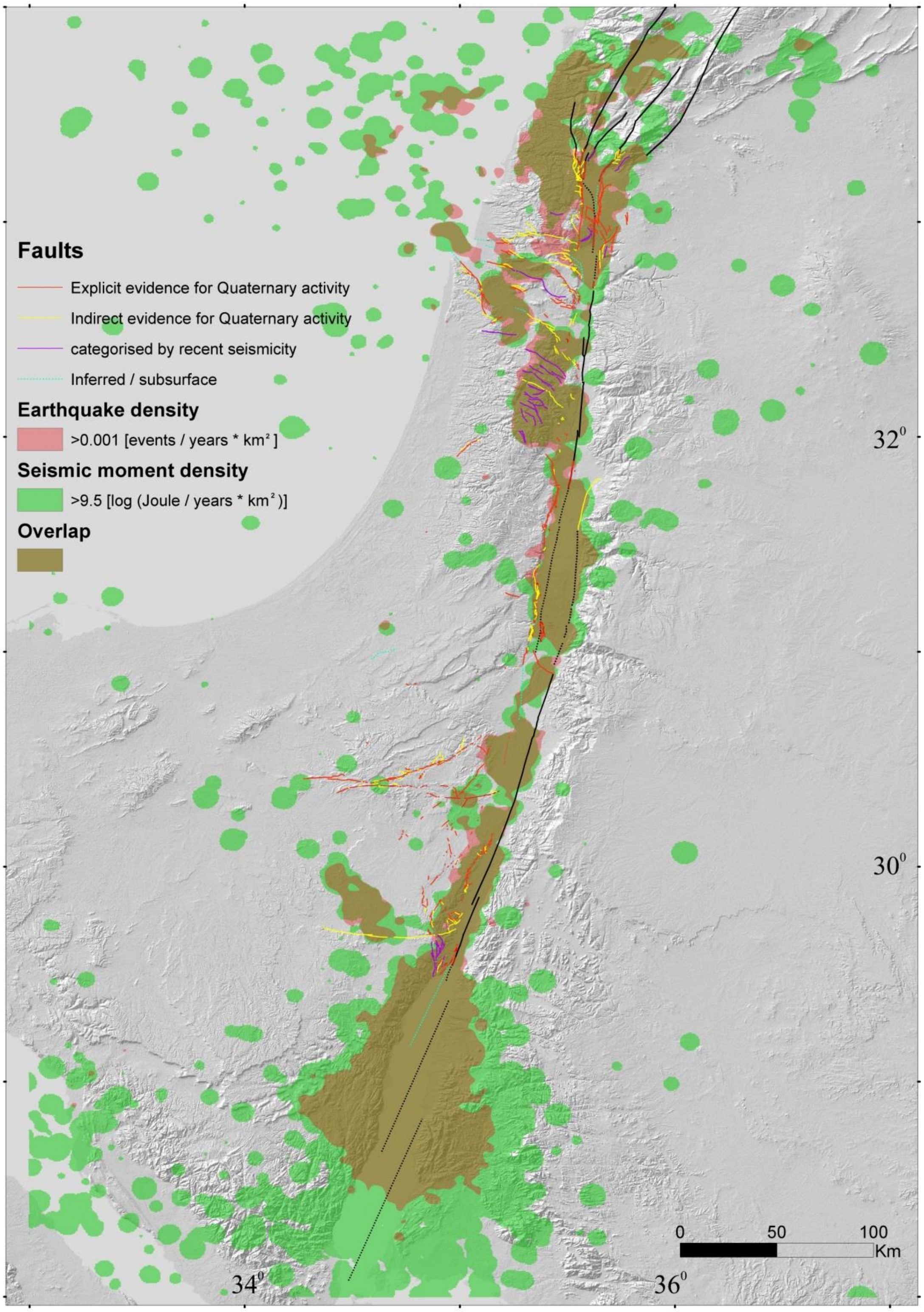
Faults
Explicit evidence for Quaternary activity
Indirect evidence for Quaternary activity
categorised by recent seismicity
Inferred / subsurface
Earthquake density
>0.001 [events / years * km²]
Seismic moment density
>9.5 [log (Joule / years * km²)]
Overlap
32°
30°
34°
36°
0
50
100
Km

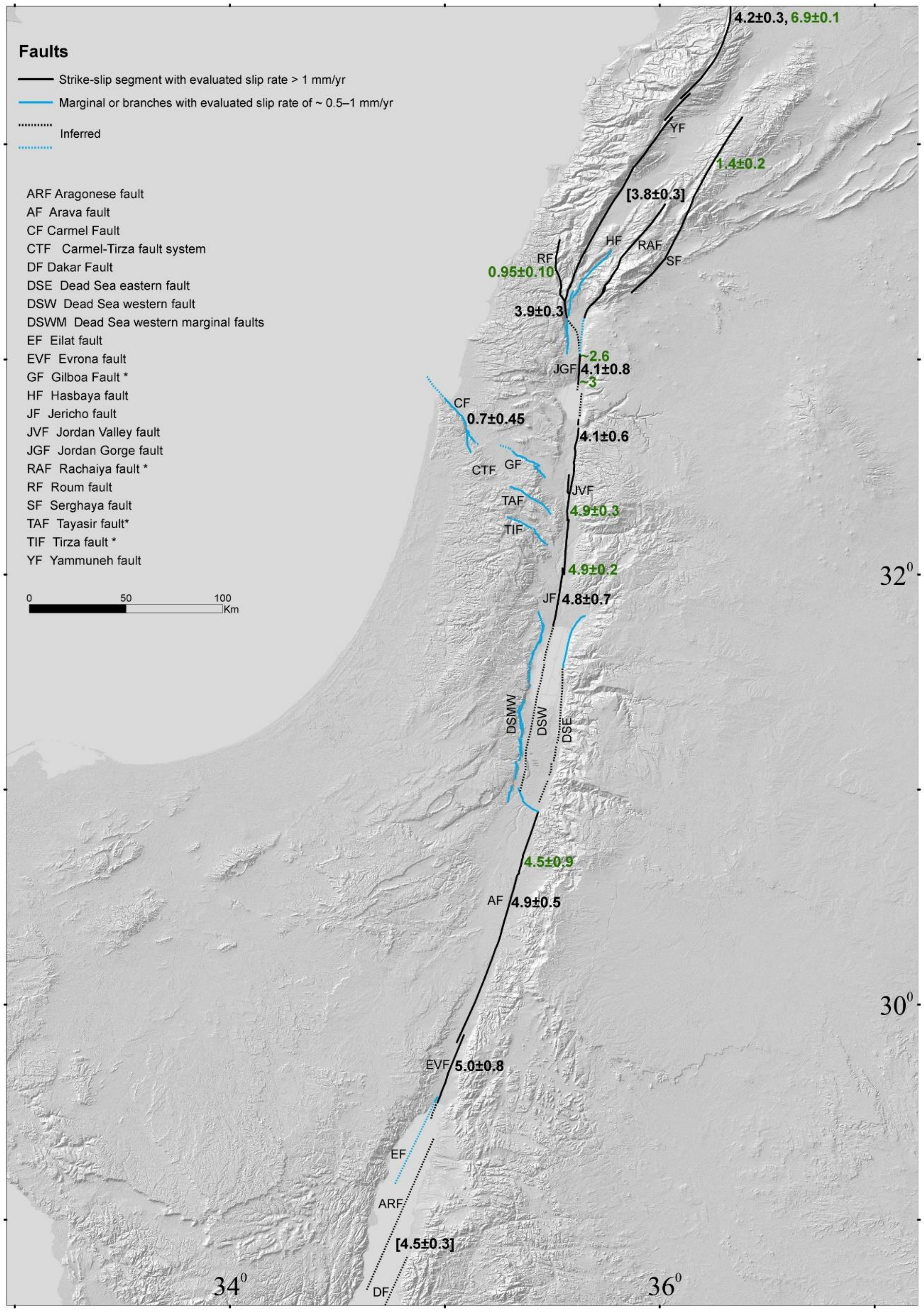

Faults
Strike-slip segment with evaluated slip rate > 1 mm/yr
Marginal or branches with evaluated slip rate of ~ 0.5–1 mm/yr
Inferred
ARF Aragonese fault
AF Arava fault
CF Carmel Fault
CTF Carmel-Tirza fault system
DF Dakar Fault
DSE Dead Sea eastern fault
DSW Dead Sea western fault
DSWM Dead Sea western marginal faults
EF Eilat fault
EVF Evrona fault
GF Gilboa Fault *
HF Hasbaya fault
JF Jericho fault
JVF Jordan Valley fault
JGF Jordan Gorge fault
RAF Rachaiya fault *
RF Roum fault
SF Serghaya fault
TAF Tayasir fault*
TIF Tirza fault *
YF Yammuneh fault
0
50
100
Km
4.2±0.3, 6.9±0.1
YF
1.4±0.2
[3.8±0.3]
HF
RAF
RF
SF
0.95±0.10
3.9±0.3
~2.6
JGF
4.1±0.8
~3
CF
0.7±0.45
4.1±0.6
CTF
GF
JVF
TAF
4.9±0.3
TIF
4.9±0.2
32⁰
JF
4.8±0.7
DSMW
DSW
DSE
4.5±0.9
AF
4.9±0.5
30⁰
EVF
5.0±0.8
EF
ARF
[4.5±0.3]
34⁰
36⁰
DF

Figure A3~~. Quaternary faults superimposed on the seismicity polygons of the seismicity-based criterion.~~

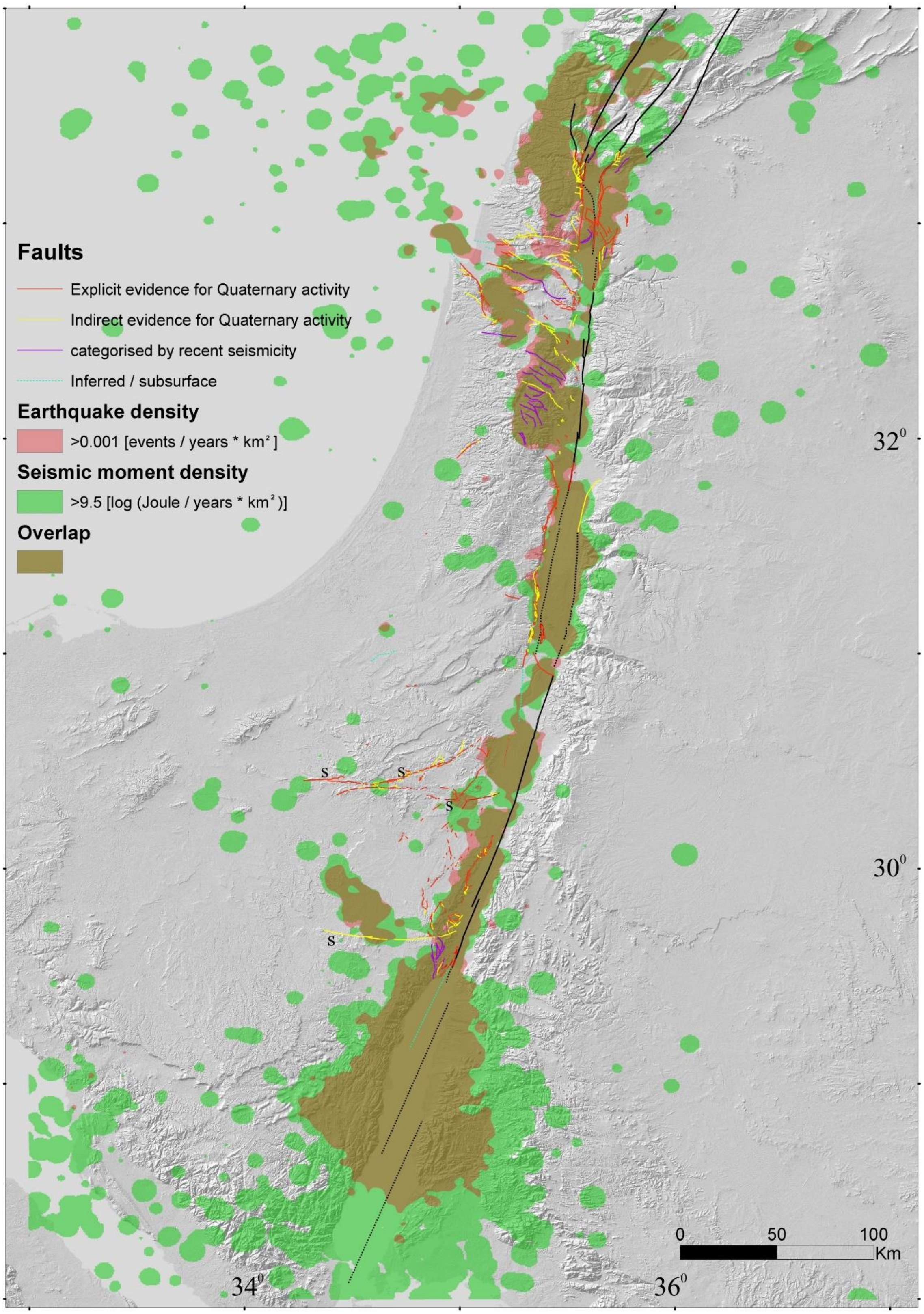
Faults
Explicit evidence for Quaternary activity
Indirect evidence for Quaternary activity
categorised by recent seismicity
Inferred / subsurface
Earthquake density
>0.001 [events / years * km²]
Seismic moment density
>9.5 [log (Joule / years * km²)]
Overlap
32°
30°
34°
36°
S
S
S
S
0
50
100
Km

Figure A4

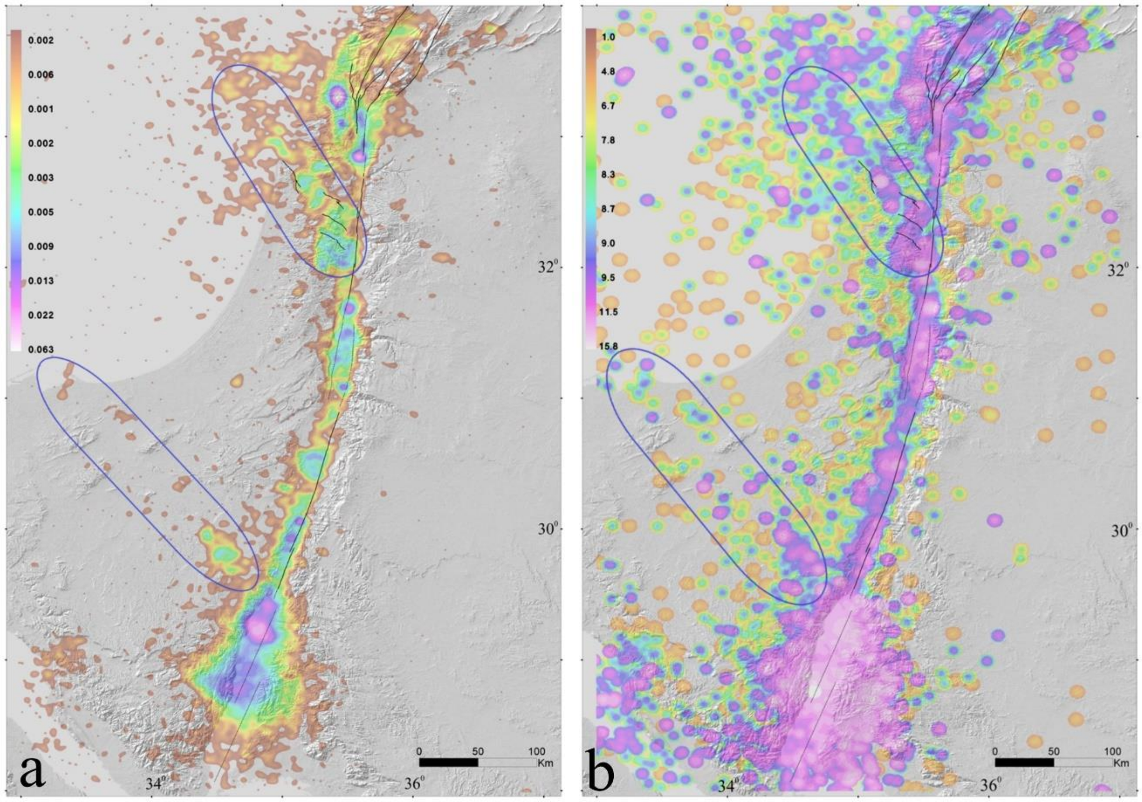

Figure A5

10. Appendix references

Avni, Y.: Paleogeography and tectonics of the Central Negev and the Dead Sea Rift western margin during the late Neogene and Quaternary, Ph.D. thesis, Hebrew University of Jerusalem, Geological Survey of Israel Report No. GSI/24/98, Jerusalem, 231 pp. (in Hebrew, English abstract), 1998.

Avni, Y., and Zilberman, E.; Landscape evolution triggered by neotectonics in the Sede Zin region, central Negev, Israel, Israel J. Earth. Sci., 55, 189–208, 2007.

Bartov, Y., Agnon, A., Enzel, Y., and Stein, M.: Late Quaternary faulting and subsidence in the central Dead Sea basin, Israel, Israel J. Earth Sci., 55, 17–32, 2006.

Ben-Avraham, Z.: Structural framework of the Gulf of Elat (Aqaba), Northern Red Sea, J. Geophys. Res., 90(B1), 703–726, 1985.

~~Ben-Avraham, Z.: Structural framework of the Gulf of Elat (Aqaba), Northern Red Sea, J. Geophys. Res., 90(B1), 703–726, 1985.~~

Ben-Avraham, Z., and Schubert, G.: Deep "drop down" basin in the southern Dead Sea, Earth Planet. Sc. Lett., 251, 254–263, 2006.

Buchbinder, B., and Sneh, A.: Marine sandstones and terrestrial conglomerates and mudstones of Neogene – Pleistocene age in the Modi'im area: a re-evaluation, Geological Survey of Israel Current Research, 1983–84, 65–69. 1984.

Calvo, R.: Stratigraphy and petrology of the Hazeva Formation in the Arava and the Negev: Implications for the development of sedimentary basins and the morphotectonics of the Dead Sea Rift Valley, Ph.D. thesis, Hebrew University of Jerusalem, Geological Survey of Israel Report No. GSI/22/02, Jerusalem, 264 pp. (in Hebrew, English abstract), 2002.

Calvo, R., Bartov, Y., Avni, Y., Garfunkel, Z., and Frislander, U.: Geological field trip to the Karkom graben: The Hazeva Fm. and its relation to the structure, Annual Meeting Field Trips Guidebook, Israel Geological Society, pp. 47–62 (in Hebrew), 1998.

Enzel, Y., Saliv, G., and Kaplan, M.: The tectonic deformation along the Zin Lineament, Nuclear Power Plant - Shivta Site: preliminary safety analysis Report. Appendix 2.5E: Late Cenozoic Geology in the Site area. Israel Electric Corporation Ltd., 1988.

Enzel, Y., Kadan, G., and Eyal, Y.: Holocene earthquakes inferred from a Fan-Delta sequence in The Dead Sea Graben, Quaternary Res., 53, 34–48, 2000.

Eppelbaum, L., Ben-Avraham, Z., and Katz, Y.: Structure of the Sea of Galilee and Kinarot Valley derived from combined geological-geophysical analysis, First Break, 25(1), 21–28, 2007.

Eyal, Y., Kaufman, A., and Bar-Matthews, M.: Use of ^{230}Th/U ages of striated Carnotites for dating fault displacements. Geology, 20, 829–832, 1992.

~~Farr, T. G., et al.: The Shuttle Radar Topography Mission, Rev. Geophys., 45, RG2004, https://doi:10.1029/2005RG000183, 2007.~~

Ferry, M., Meghraoui, M., Abou Karaki, N., Al-Taj, M., Amoush, H., Al-Dhaisat, S., and Barjous, M.: A 48-kyr-long slip rate history for the Jordan Valley segment of the Dead Sea Fault, Earth Planet. Sc. Lett., 260, 394–406, 2007.

Garfunkel, Z.: Lateral motion and deformation along the Dead Sea transform, in: Dead Sea Transform Fault System: Reviews, edited by: Garfunkel, Z., Ben-Avraham, Z., and Kagan, E. J., Springer, Dordrecht, the Netherlands, 109–150, 2014.

Ginat, H.: Paleogeography and the landscape evolution of the Nahal Hiyyon and Nahal Zihor basins, Ph.D. thesis, Hebrew University of Jerusalem, Geological Survey of Israel Report No. GSI/19/97, Jerusalem, 206 pp. (in Hebrew, English abstract), 1997.

Hartman, G., Niemi, T. M., Tibor, G., Ben-Avraham, Z., Al-Zoubi, A., Makovsky, Y., Akawwi, E., Abueladas, A.-R., and Al-Ruzouq, R.: Quaternary tectonic evolution of the Northern Gulf of Elat/Aqaba along the Dead Sea Transform, J. Geophys. Res.: Solid Earth, 119, 9183–9205, doi:10.1002/2013JB010879, 2014.

Hurwitz, S., Garfunkel, Z., Ben-Gai, Y., Reznikov, M., Rotstein, Y., and Gvirtzman, H.: The tectonic framework of a complex pull-apart basin: seismic reflection observations in the Sea of Galilee, Dead Sea transform. Tectonophysics, 359(3-4), 289-306, 2002.

IEC and WLA (Israel Electric Corporation and William Lettis & Associates, Inc.): Shivta-Rogem Site Report. Israel Electric Corporation, Ltd., 2002.

Kafri, U., and Ecker, A.: Neogene and Quaternary subsurface geology and hydrogeology of the Zevulun plain, Geological Survey of Israel Bulletin No. 37, Jerusalem, 13 pp., 1964.

Katz, O., Amit, R., Yagoda-Biran, G., Hatzor, Y. H., Porat, N., and Medvedev, B.: Quaternary earthquakes and landslides in the Sea of Galilee area, the Dead Sea Transform: paleoseismic analysis and implication to the current hazard, Israel J. Earth. Sci., 58, 275–294, 2009.

Le Béon, M., Klinger, Y., Mériaux, A.-S., Al-Qaryouti, M., Finkel, R. C., Mayyas, O., and Tapponnier, P.: Quaternary morphotectonic mapping of the Wadi Araba and implications for the tectonic activity of the southern Dead Sea fault. Tectonics, 31, TC5003, doi:10.1029/2012TC003112, 2012.

Marco, S., Hartal, M., Hazan, N., Lev, L. and Stein, M.: Archaeology, history and Geology of the A.D. 749 earthquake, Dead Sea transform, Geology, 31, 665– 668, 2003.

Mitchell, S. G., Matmon, A., Bierman, P. R., Enzel, Y., Caffee, M., and Rizzo, D.: Displacement history of a limestone normal fault scarp, northern Israel, from cosmogenic ^{36}Cl, J. Geophys. Res., 106(B3), 4247–4264, 2001.

Reznikov, M., Ben-Avraham, Z., Garfunkel, Z., Gvirtzman, H., and Rotstein, Y.: Structural and stratigraphic framework of Lake Kinneret, Israel J. Earth. Sci., 53, 131–149, 2004.

Sagy, A., and Nahmias, Y.: Characterizing active faulting zone, in: Infrastructure instability along the Dead Sea: Final Report: 2008–2010, edited by: Baer, G., Geological Survey of Israel Report No. GSI/02/2011, Jerusalem, 7–17 (in Hebrew), 2011.

Sagy, Y., and Gvirtzman, Z.: Subsurface mapping of the Zevulun valley, The Geophysical Institute of Israel Report 648/454/09, Lod, 21 pp. (in Hebrew), 2009.

Schattner, U., and Ben-Avraham, Z.: Transform margin of the northern Levant, eastern Mediterranean: From formation to reactivation, Tectonics, 26, TC5020, doi:10.1029/2007TC002112, 2007.

Schattner, U., and Weinberger, R.: A mid-Pleistocene deformation transition in the Hula basin, northern Israel: Implications for the tectonic evolution of the Dead Sea Fault, Geochem. Geophys. Geosyst., 9(7), Q07009, doi: 10.1029/2007GC001937, 2008.

Sneh, A., and Weinberger, R.: Major geological structures of Israel and Environs, Geological Survey of Israel, Jerusalem, 2014.

Weinberger, R., Gross, M. R., and Sneh, A.: Evolving deformation along a transform plate boundary: Example from the Dead Sea Fault in northern Israel, Tectonics, 28, TC5005, doi:10.1029/2008TC002316, 2009.

Wieler, N., Avni, A., Ginat, H., and Rosensaft, M.: Quaternary map of the Eilat region on a scale of 10:000 with explanatory notes, Geological Survey of Israel Report No. GSI/37/2016, Jerusalem, 15 pp. (in Hebrew, English abstract), 2017.

Zilberman, E.: The geology of the central Sinai-Negev shear zone, central Negev. Part C: The Paran Lineament, Geological Survey of Israel Report No. GSI/38/85, Jerusalem, 53 pp., 1985.

Zilberman, E., Baer. G., Avni, Y., and Feigin, D.: Pliocene fluvial systems and tectonics in the central Negev, southern Israel, Israel J. Earth. Sci., 45, 113–126, 1996.

Zilberman, E., Greenbaum, N., Nahmias, Y., Porat, N., and Ashqar, L.: Middle Pleistocene to Holocene tectonic activity along the Carmel Fault - preliminary results of a paleoseismic study, Geological Survey of Israel Report No. GSI/02/2007, Jerusalem, 35 pp., 2006.

Zilberman, E., Greenbaum, N., Nahmias, Y., Porat, N., and Ashkar, L.: Late Pleistocene to Holocene tectonic activity along the Nesher fault, Mount Carmel, Israel, Israel J. Earth. Sci., 57, 87–100, 2008.

Zilberman, E., Nahmias, Y., Gvirtzman, Z., and Porat, N.: Evidence for late Pleistocene and Holocene tectonic activity along the Bet Qeshet fault system in the Lower Galilee, Geological Survey of Israel Report No. GSI/06/2009, Jerusalem, 22 pp. (in Hebrew, English abstract), 2009.

Zilberman, E., Ron, H., Sa'ar, R.: Evaluating the potential seismic hazards of the Ahihud Ridge fault system by paleomagnetic and morphological analyses of calcretes, Geological Survey of Israel Report No. GSI/15/2011, Jerusalem, 30 pp., 2011.